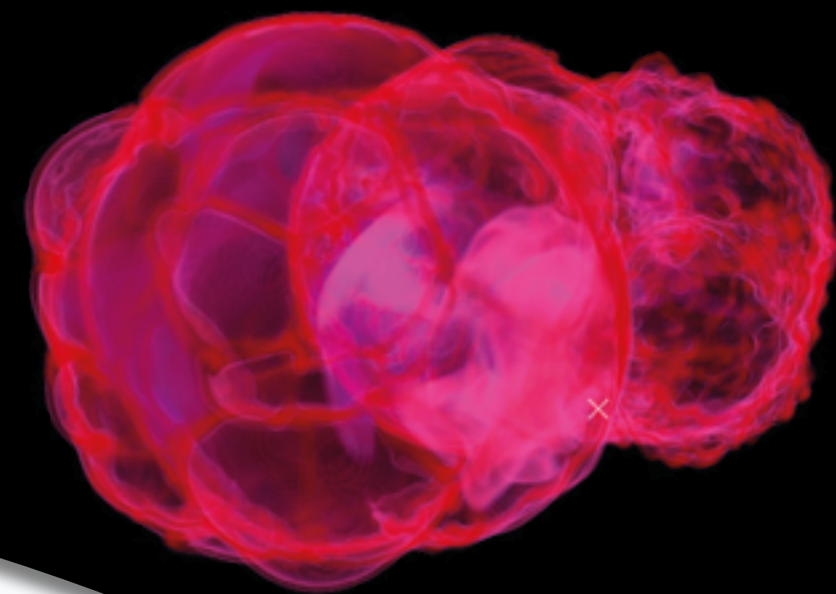

Assessing the link between recent supernovae near Earth and the iron-60 anomaly in a deep-sea crust

<u>Michael M. Schulreich</u>

Dieter Breitschwerdt

In collaboration with:
Jenny Feige (also TU Berlin)
Christian Dettbarn (ARI Heidelberg)

Supernova remnants – an odyssey in space after stellar death
9 June 2016, Chania, Crete, Greece

Recovery of the ferromanganese (FeMn) crust sample 237KD from the equatorial Pacific floor in 1976

Image credits: Google Maps (background), http://www.oceanexplorer.noaa.gov (top right photo), D. Quadfasel (all other photos)

Motivation — Relics of a 'Blast from the Past'?

- Each crust layer corresponds to certain age range
- Knie et al. (2004) detected significant abundance increase of radioisotope ^{60}Fe in ~2.2 Myr-old layer; signal confirmed by Fitoussi et al. (2008)

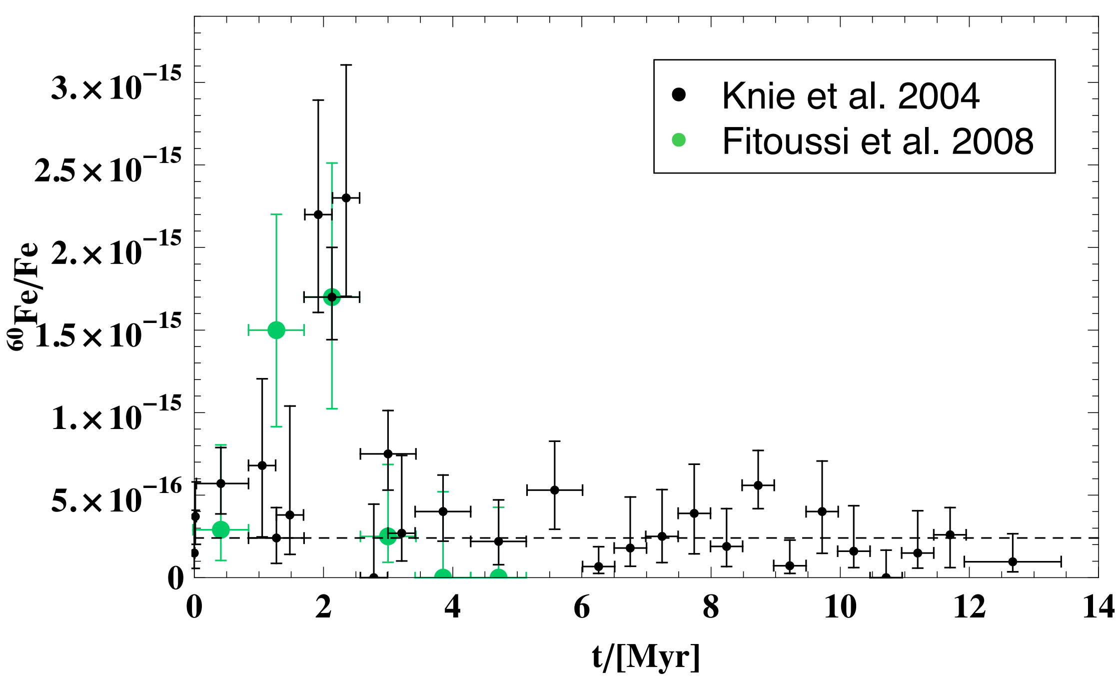

What's so special about ^{60}Fe?

- Produced during late shell-burning phase in massive stars; predominantly released by core-collapse SNe (cf. Knödlseder et al. 2004)
- Low terrestrial background
- Comparatively long half-life ($\tau_{1/2}$ ~ 2.62 Myr) allows for extensive ISM travelling ➔ detectable by β^- decay via ^{60}Co and γ-ray emission at 1173 and 1333 keV (Wang et al. 2007)

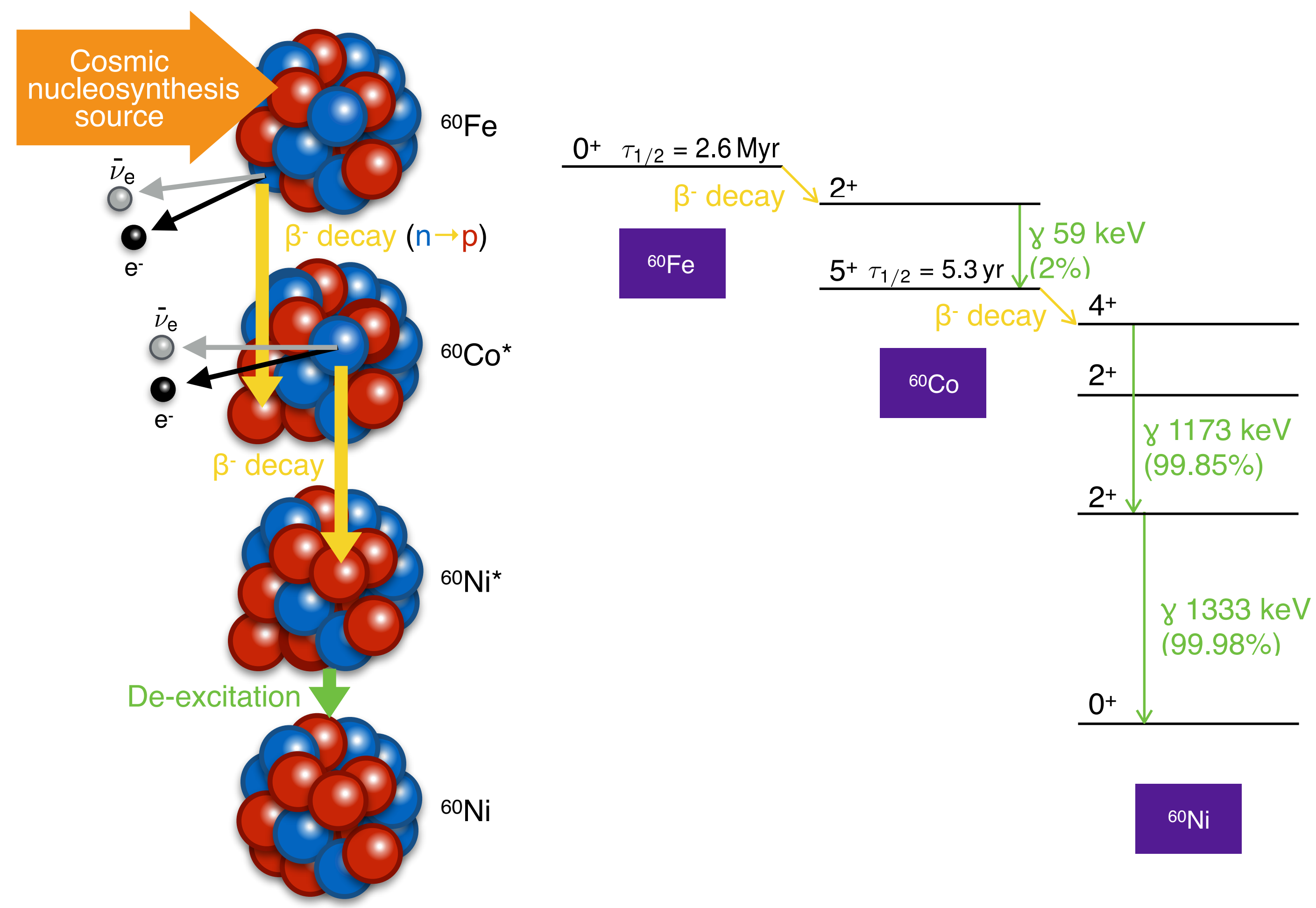

- Link between the ^{60}Fe anomaly and recent SNe near Earth that also contributed to the formation of the **Local Bubble** (LB)

Background — The Local Bubble

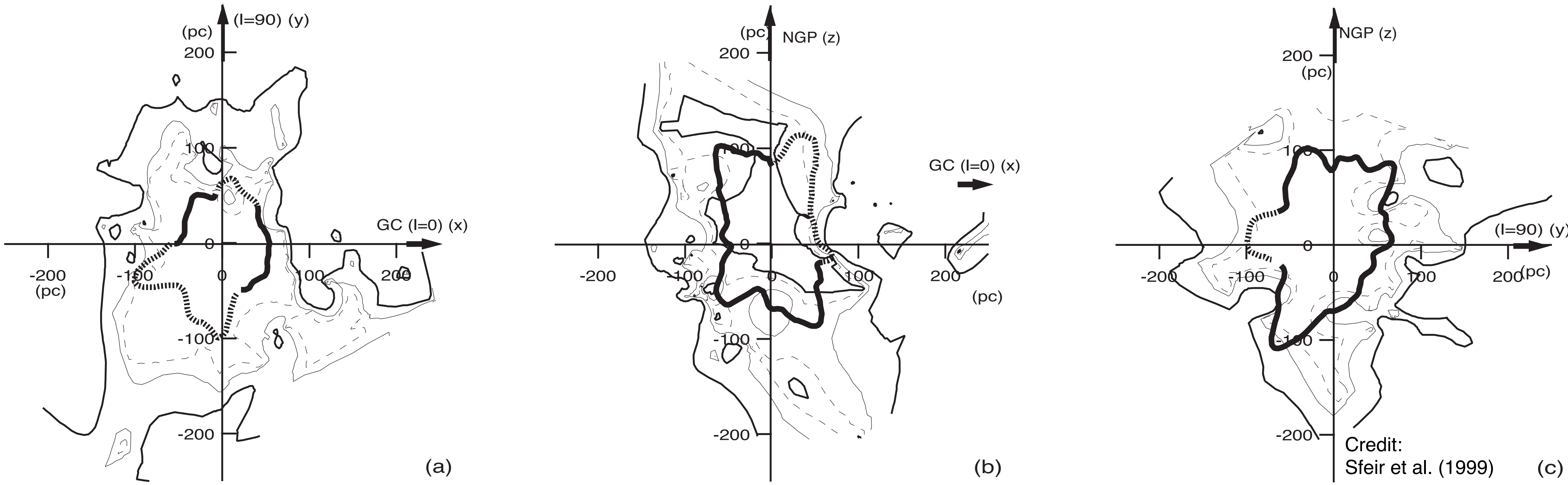

- Our Galactic habitat
- Low-density region of the ISM
- Partially filled with hot, soft X-ray emitting gas
  - Responsible for ~60% of the 0.25-keV flux in the Galactic plane (Galeazzi et al. 2014) ➔ **bold confirmation of its existence**
- **Size:** ~200 pc in the Galactic plane; ~600 pc perpendicular to it (chimney?)
- **Widely accepted origin:** several nearby SN explosions in the last ~10 Myr (e.g., Smith & Cox 2001)
  - But, **no young stellar cluster** could be found inside its boundaries

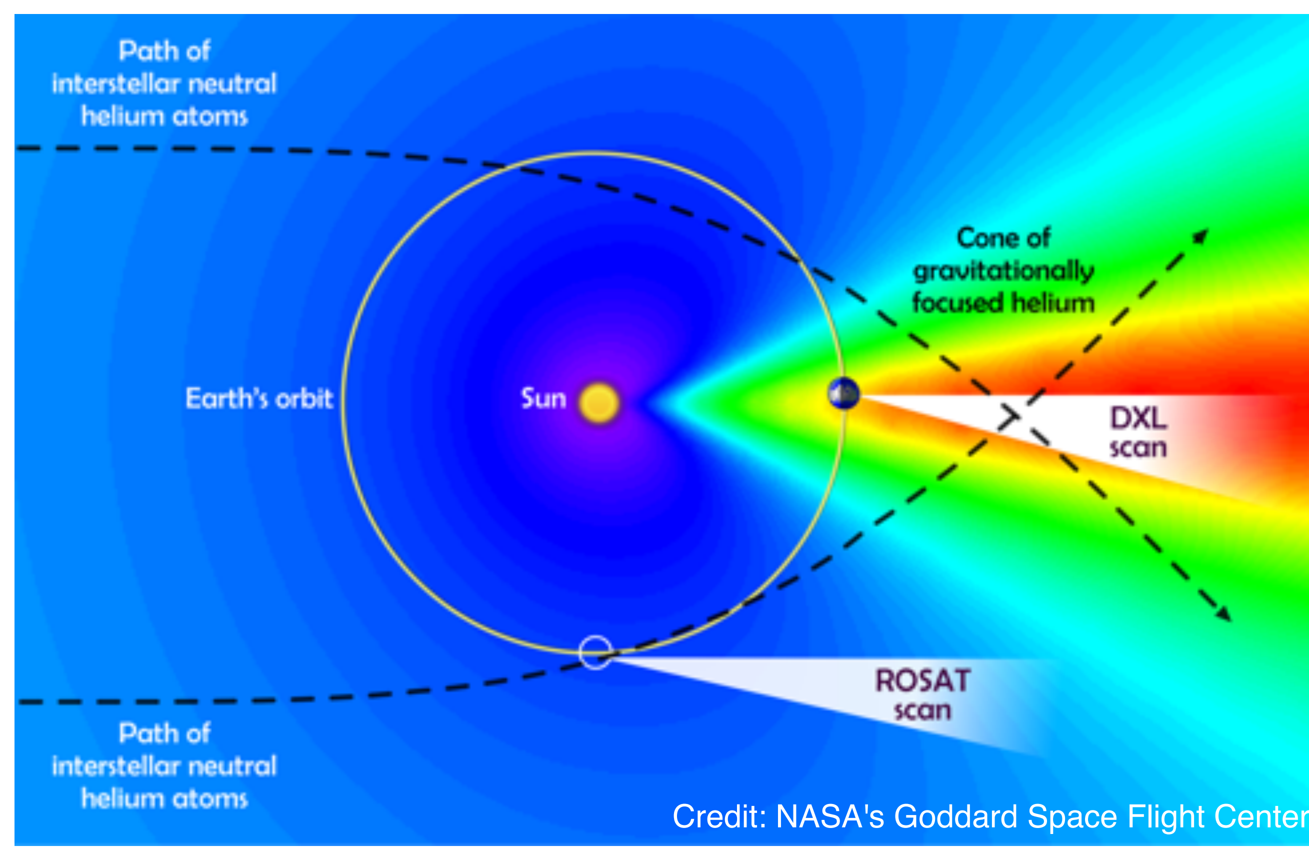

Background — The Local Bubble

- Fuchs et al. (2006) analyzed volume complete sample (D ~ 400 pc) centered at the solar system in the HIPPARCOS and ARIVEL catalogues
- Selected only those 79 B stars that are concentrated in both real and velocity space
- Extrapolated trajectories (center of mass) back in space & time
- Applied initial mass function (IMF) ➔ **number of SNe in the past**; **explosion sites** (from trajectories); **explosion times** (from MS life times; assuming that stars in cluster are born coevally)
- Cluster age: put de-reddened cluster stars into CMD; turn-off point from isochrones (Schaller 1992)
- Association entered present LB volume rather off-centre 10–15 Myr ago
- Since then, 14–20 SN explosions should have occurred
- Corresponding energy input into surrounding ISM is consistent with current LB size
- Scenario further tested by means of 3D hydrodynamical simulations ➔ matching extension & ion column density ratios (Breitschwerdt & de Avillez 2006 [BA06]; de Avillez & Breitschwerdt 2009, 2012)
- **Additional constraints from FeMn crust measurements!**

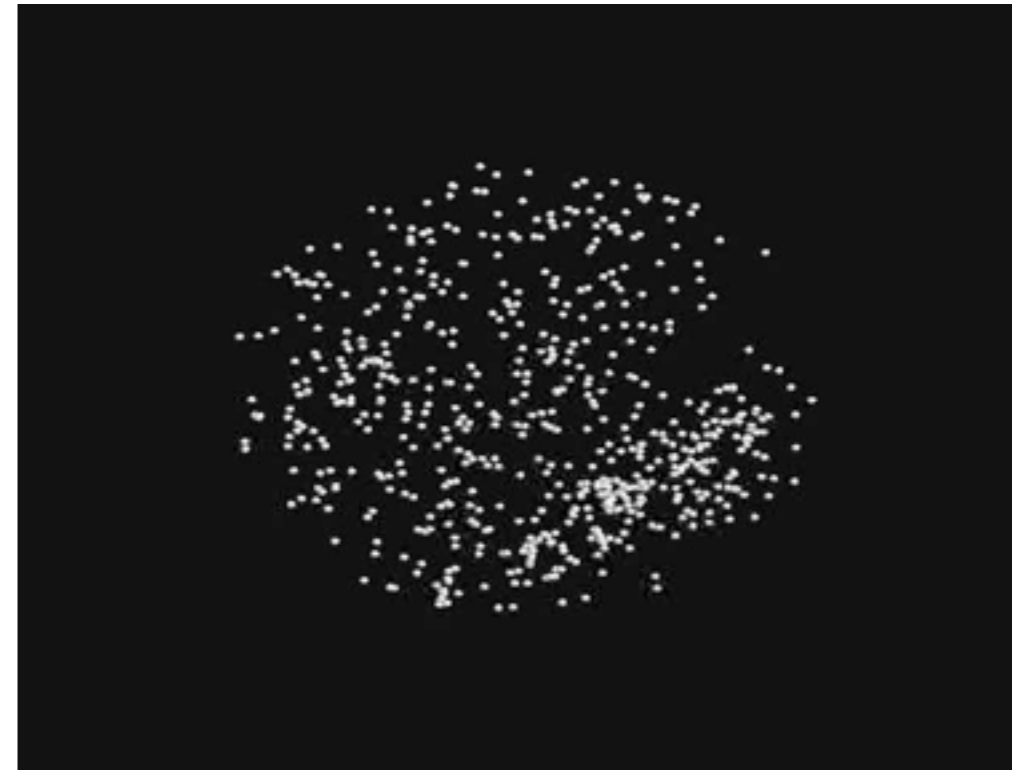

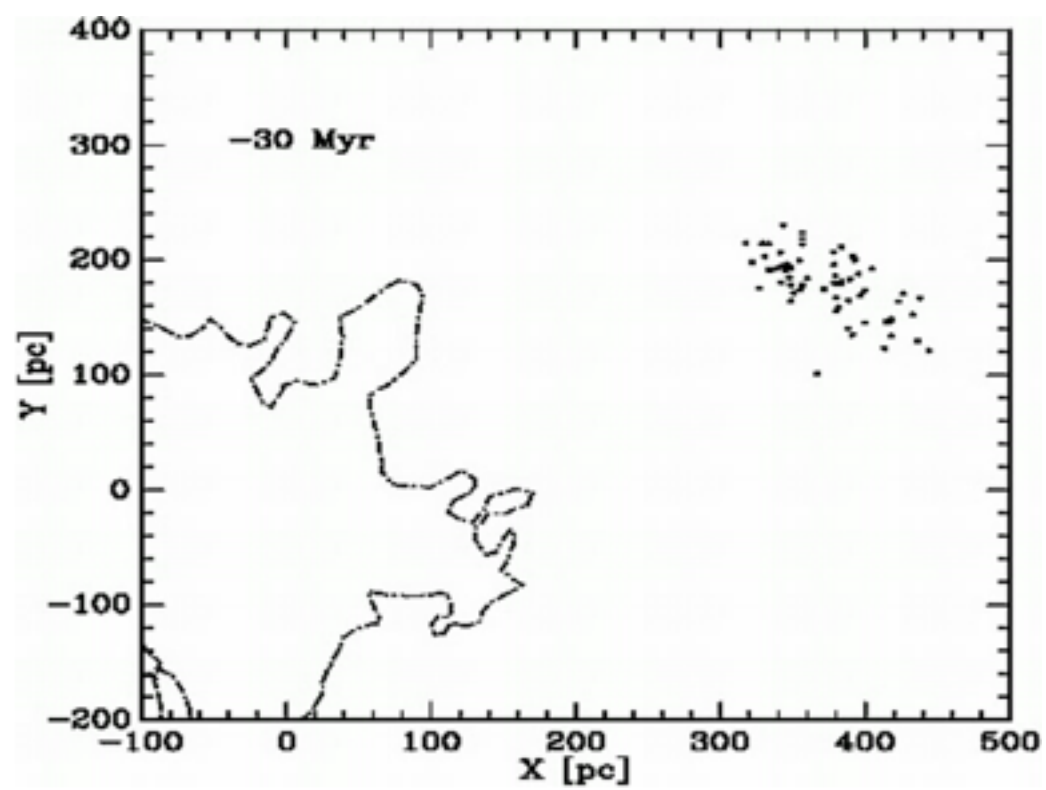

Credit: Fuchs et al. (2006)

Background — The Local Bubble

- Fuchs et al. (2006) analyzed volume complete sample (D ~ 400 pc) centered at the solar system in the HIPPARCOS and ARIVEL catalogues
- Selected only those 79 B stars that are concentrated in both real and velocity space
- Extrapolated trajectories (center of mass) back in space & time
- Applied initial mass function (IMF) ➔ **number of SNe in the past**; **explosion sites** (from trajectories); **explosion times** (from MS life times; assuming that stars in cluster are born coevally)
- Cluster age: put de-reddened cluster stars into CMD; turn-off point from isochrones (Schaller 1992)
- Association entered present LB volume rather off-centre 10–15 Myr ago
- Since then, 14–20 SN explosions should have occurred
- Corresponding energy input into surrounding ISM is consistent with current LB size
- Scenario further tested by means of 3D hydrodynamical simulations ➔ matching extension & ion column density ratios (Breitschwerdt & de Avillez 2006 [BA06]; de Avillez & Breitschwerdt 2009, 2012)
- **Additional constraints from FeMn crust measurements!**

Analytical study by Feige (2010)

- Basis: Fuchs et al. data & SN model by Kahn (1998)
- SNR does not expand into homogeneous medium, but into a medium that has already been shaped by previous SN events ($\rho = \Omega r^n$ with $n = 9/2$)
- The radius of the expanding SNR evolves as $r_s^{n+5} = \frac{(n+5)(2n+7)}{6\pi} \frac{E_{SN} t^2}{\Omega}$
- ^{60}Fe yields taken as a function of the massive stars' initial masses from stellar evolution models
  - ^{60}Fe amount deposited on Earth by arriving SN blast waves
  - Good agreement with crust measurements

Model restrictions:

- Ambient medium is either homogeneous (see, e.g., Fry et al. 2015) or with power-law density distribution; external pressure must be small compared to pressure in bubble interior
- External medium taken to be constant for all but the very first explosion
- Turbulent mixing and mass loading not incorporated

Overcoming these shortcomings requires …

- performing 3D high-res. numerical simulations
- using self-consistently evolved turbulent ISM as a typical background medium (like [BA06])

Method — RAMSES: a parallel graded octree AMR CFD code

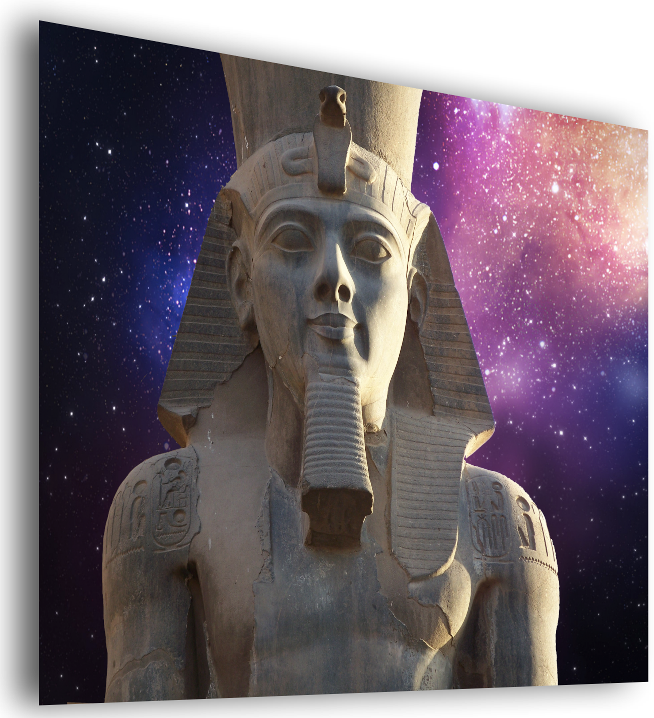

- Code developed by Teyssier (2002)
- Freely available for download online
- **Tree-based AMR** (octree structure): Cartesian mesh is recursively refined on cell-by-cell basis
- **Fully threaded:** each oct has direct access to neighboring parent cells and children octs ➔ Optimized mesh adaption to complex geometries
- **MPI-based** parallel implementation ➔ Space filling curves

- **Hydro module:** Unsplit second-order Godunov method ➔ Riemann solver with piecewise linear reconstruction (MUSCL-Hancock scheme)
- **N body module:** Particle-mesh method on AMR grids; efficient Poisson solvers (e.g., Multigrid)
- **MHD module:** Constrained transport scheme
- **RHD module:** GPU-accelerated (CUDA libraries); grey flux-limited diffusion approximation
- Additional physical modules mainly tailored for cosmological applications

Modified and extended RAMSES to perform meso-scale ISM simulations:

- Star formation (IMF; collisionless particles represent massive stars) at Gal. rate
- Feedback from stellar winds and SNe
- Solar wind bubble
- Self-gravity of the gas & Galactic gravitational potential
- Heating & CIE cooling for gas with solar metallicity (using CLOUDY code)
- Stellar trajectories (provided by Ch. Dettbarn): UCL/LCC (Sco-Cen subgroups)
  - Take errors in Hipparcos data into account
  - Drop assumption of center of mass motion for all SN precursors
  - Use Gaussian error distribution for stellar paths

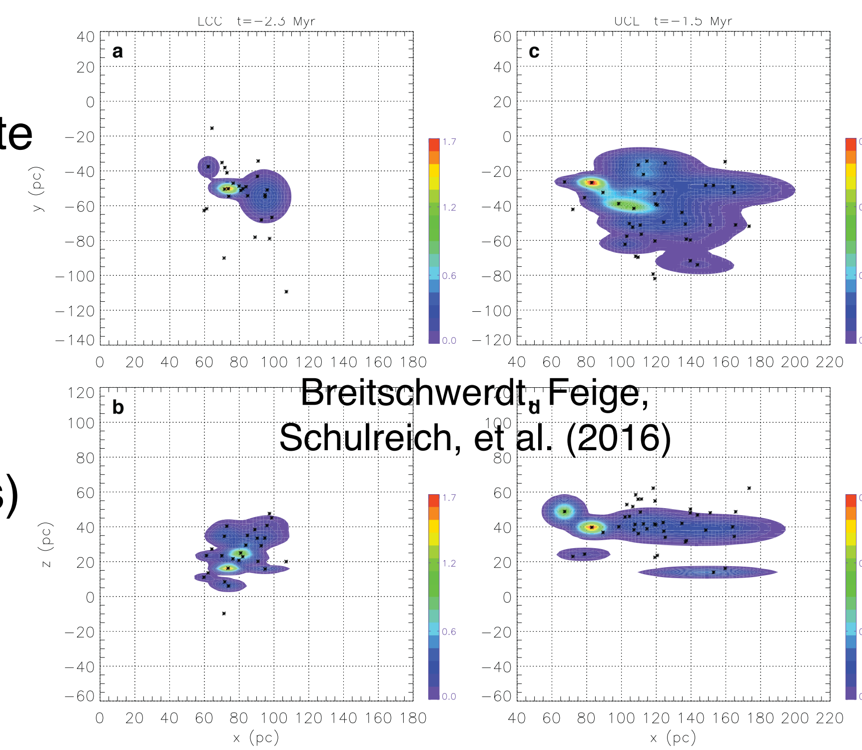

Breitschwerdt, Feige, Schulreich, et al. (2016)

Method — Additional model parameters and assumptions

	Homogeneous background models (A & B)	Inhomogeneous background model (C)
Box size	3 x 3 x 3 kpc^3	3 x 3 x 3 kpc^3
Highest grid resolution	0.7 pc (ℓ_{max} = 12)	2.9 pc (ℓ_{max} = 10)
Boundary conditions (vertical faces / top and bottom)	periodic / periodic	periodic / outflow
Total evolution time	12.6 Myr	192.6 Myr (180 + 12.6 Myr)
Initial gas distribution	homogeneous	analytical fit to observational data of the Galaxy (Ferrière 1998)
External gravitational field	no	yes
Self-gravity	yes	no

- Neglect any initial radial gradients (in analytical functions, set $R = R_\odot$)
- Assume that computational box corotates with Local Standard of Rest ➔ *'justified'* by usually small peculiar motions of interstellar gas
- Neglect shear due to differential Galactic rotation ➔ *'justified'* for LB formation scenario: paths of progenitor stars are almost parallel to *y*-axis

Method — Modeling the Loop I superbubble

- ROSAT PSPC observations (Egger & Aschenbach 1995) revealed that SXRs are absorbed by nearby neutral shell
  - Possibly the result of an **interaction between the LB and its neighbouring SB Loop I** (Breitschwerdt et al. 2000)
  - **Study joint evol. of LB & Loop** (like Breitschwerdt & de Avillez 2006)
- Ch. Dettbarn (priv. comm.) searched in Sun-centered sphere ($D = 800$ pc) for Loop I progenitor stars
  - Tr 10 and the Vel OB2 association have recently passed through the present volume of Loop I
  - $\mathcal{N} \sim 80$ stars entered this volume $\Delta\tau \sim 12.3$ Myr ago
- **How many stars have already exploded?**
  - Use IMF for young massive stars (Massey et al. 1995):
    $$\frac{d\mathcal{N}}{dM} = \left.\frac{d\mathcal{N}}{dM}\right|_0 M^{\Gamma-1} \quad (\Gamma = -1.1 \pm 0.1)$$
  - Relevant mass range is defined by A0 ($M_\ell = 2.6\ \mathrm{M}_\odot$) and B0 stars ($M_u = 8.2\ \mathrm{M}_\odot$) ➔ normalisation constant
    $$\left.\frac{d\mathcal{N}}{dM}\right|_0 = \mathcal{N}\left[\int_{2.6}^{8.2} M^{-2.1}\, dM\right]^{-1} = 351$$
  - Lifetime of the first and most massive star that exploded in Loop I:
    $\tau_{M_{\Delta\tau}} = \tau_u - \Delta\tau$ ➔ mass
    $$M_{\Delta\tau} = \left(M_u^{-\beta} - \frac{\Delta\tau}{\tau_0}\right)^{-1/\beta} = 19.2\,\mathrm{M}_\odot$$
    ($\beta = 0.932$, $\tau_0 = 1.6 \times 10^8$ yr)
  - Number of missing stars (LB: 16)
    $$\mathcal{N}_{\mathrm{SN}} = \int_{8.2}^{19.2} \left.\frac{d\mathcal{N}}{dM}\right|_0 M^{-2.1}\, dM = 19$$
- **Statistically most probable mass distribution:** perform mass binning by assigning exactly one star to each IMF mass interval (take average mass of each bin)
- **Explosion times:** $t_{\mathrm{exp}} = \tau - \tau_{\mathrm{c}}$ ($\tau_{\mathrm{c}} = 23$ Myr: cluster age)
- **Explosion centers:** use progenitor stars' most probable (pseudo-) trajectories (based on HIPPARCOS positions and proper motions & radial velocities from various sources; probabilities take into account the errors of the corresponding individual input velocities; Credit: Chr. Dettbarn)
- **Total ejected mass** (M_{ej}) & **^{60}Fe mass fractions** (Z): fit stellar evolution models

Credit: Breitschwerdt et al. (2000)

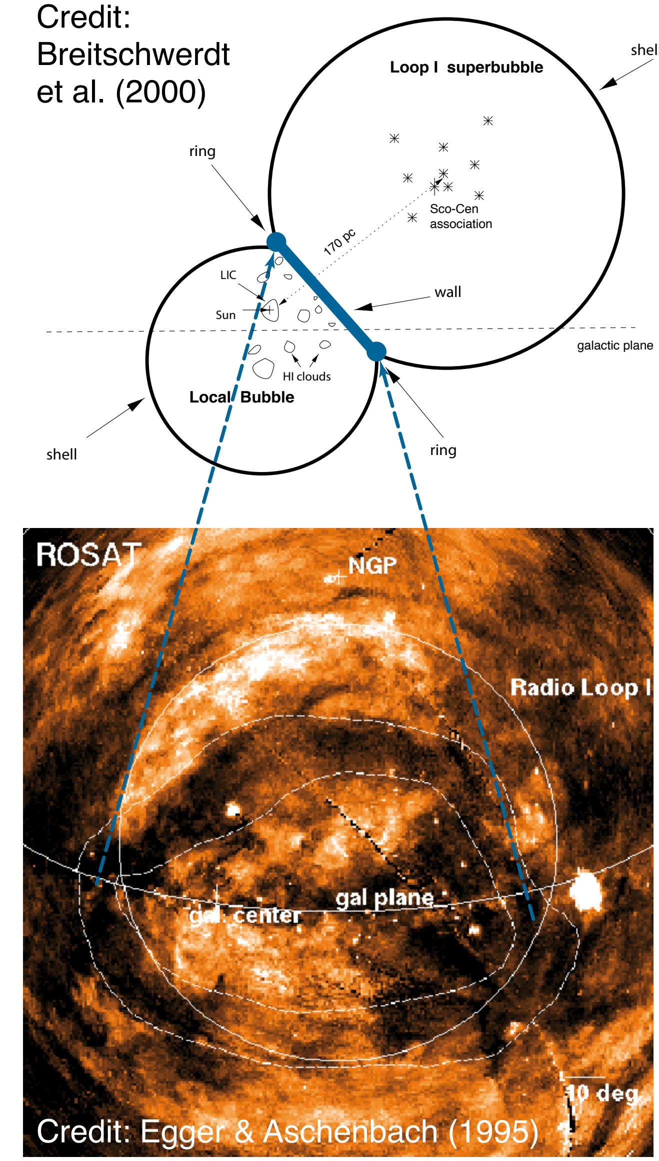

Credit: Egger & Aschenbach (1995)


Credit: DLR

Method — Modeling the Loop I superbubble

- ROSAT PSPC observations (Egger & Aschenbach 1995) revealed that SXRs are absorbed by nearby neutral shell
  - Possibly the result of an **interaction between the LB and its neighbouring SB Loop I** (Breitschwerdt et al. 2000)
  - **Study joint evol. of LB & Loop** (like Breitschwerdt & de Avillez 2006)
- Ch. Dettbarn (priv. comm.) searched in Sun-centered sphere ($D = 800$ pc) for Loop I progenitor stars
  - Tr 10 and the Vel OB2 association have recently passed through the present volume of Loop I
  - $\mathcal{N} \sim 80$ stars entered this volume $\Delta\tau \sim 12.3$ Myr ago
- **How many stars have already exploded?**
  - Use IMF for young massive stars (Massey et al. 1995):
    $$\frac{d\mathcal{N}}{dM} = \left.\frac{d\mathcal{N}}{dM}\right|_0 M^{\Gamma-1} \quad (\Gamma = -1.1 \pm 0.1)$$
  - Relevant mass range is defined by A0 ($M_\ell = 2.6\,M_\odot$) and B0 stars ($M_u = 8.2\,M_\odot$) ➔ normalisation constant
    $$\left.\frac{d\mathcal{N}}{dM}\right|_0 = \mathcal{N}\left[\int_{2.6}^{8.2} M^{-2.1}\,dM\right]^{-1} = 351$$
  - Lifetime of the first and most massive star that exploded in Loop I:
    $\tau_{M_{\Delta\tau}} = \tau_u - \Delta\tau$ ➔ mass
    $$M_{\Delta\tau} = \left(M_u^{-\beta} - \frac{\Delta\tau}{\tau_0}\right)^{-1/\beta} = 19.2\,M_\odot$$
    ($\beta = 0.932$, $\tau_0 = 1.6 \times 10^8$ yr)
  - Number of missing stars (LB: 16)
    $$\mathcal{N}_{SN} = \int_{8.2}^{19.2} \left.\frac{d\mathcal{N}}{dM}\right|_0 M^{-2.1}\,dM = 19$$
- **Statistically most probable mass distribution:** perform mass binning by assigning exactly one star to each IMF mass interval (take average mass of each bin)
- **Explosion times:** $t_{exp} = \tau - \tau_c$ ($\tau_c = 23$ Myr: cluster age)
- **Explosion centers:** use progenitor stars' most probable (pseudo-) trajectories (based on HIPPARCOS positions and proper motions & radial velocities from various sources; probabilities take into account the errors of the corresponding individual input velocities; Credit: Chr. Dettbarn)
- **Total ejected mass** (M_{ej}) & **^{60}Fe mass fractions** (Z): fit stellar evolution models

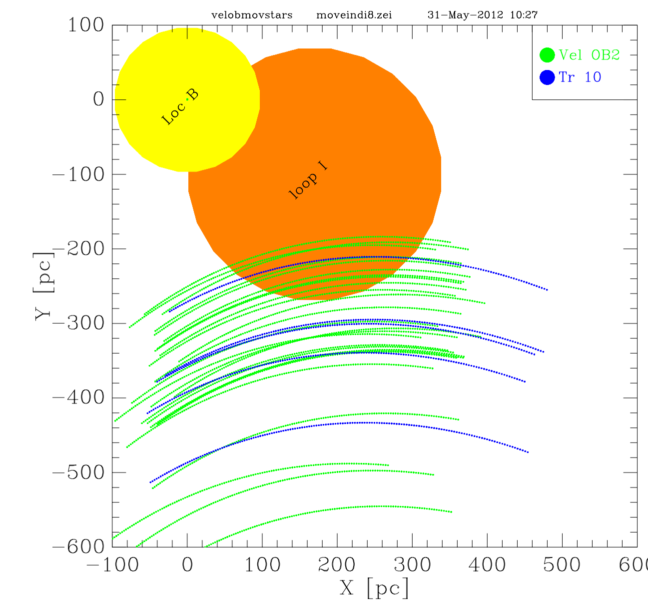

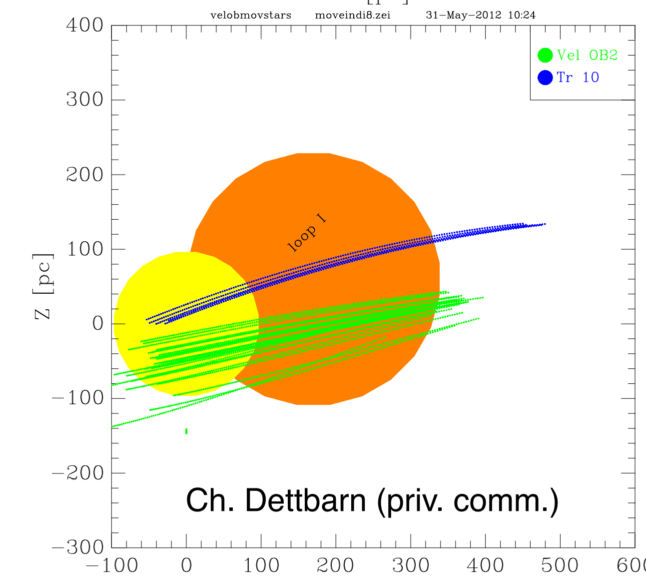

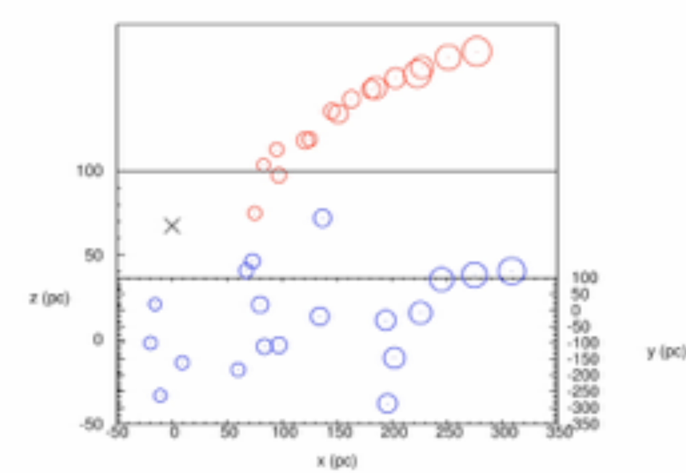

Method — Calculating the amount of SN-released ^{60}Fe that arrives on Earth

- ^{60}Fe yields depend on stellar masses
- Treat spatiotemporal evolution of the concentration of ^{60}Fe (chemical mixing) as advection-diffusion process of passive scalar(s)
- Implementation includes radioactive decay of ^{60}Fe based on the latest half-life data

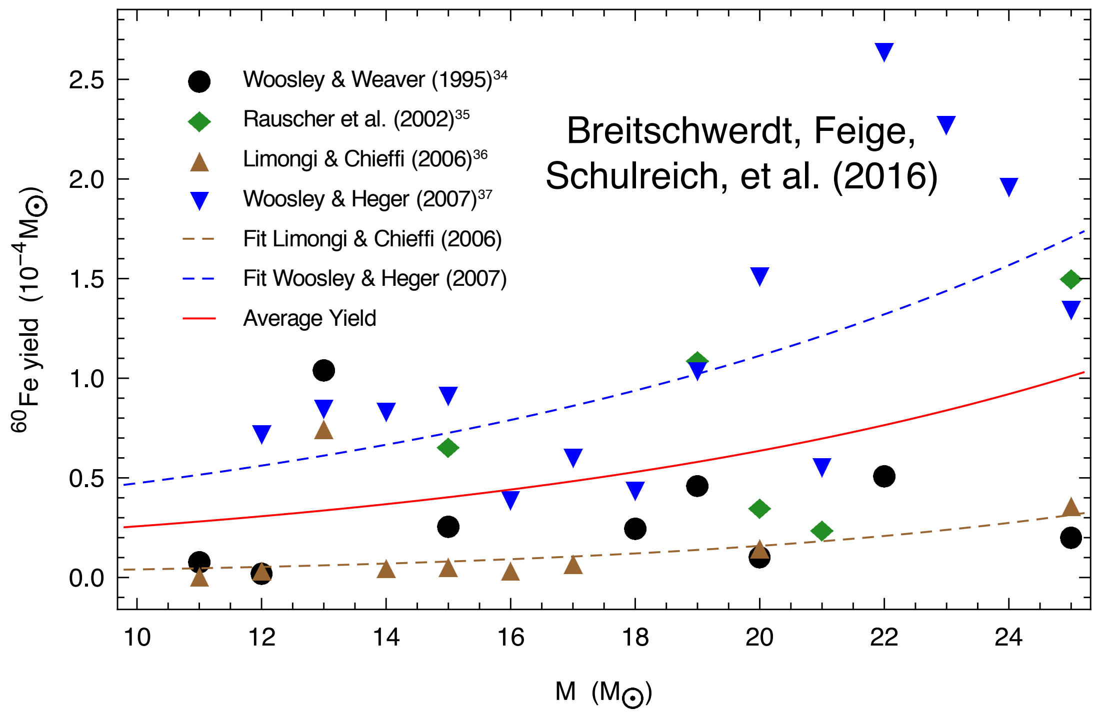

1. Force maximum grid refinement in the region of the solar system ➔ allow for accurate ^{60}Fe flux measurements in every single time step
2. As fluxes are given at cell centers: average over eight innermost grid cells
3. Compute time-integrated flux ('fluence'): $F = \frac{\rho|\mathbf{u}|Z}{Am_p}\Delta t$
4. Use F to calculate surface density of atoms deposited on Earth at time t before present: $\Sigma(t) = \frac{fU}{4} F \exp\left(-t/\tau_{1/2}\right)$
   - Assume isotropic fall-out (cf. Fry et al. 2016)
   - Components of **^{60}Fe survival fraction**, fU, only poorly known; dust factor $f \simeq 0.01$ (Fry et al. 2015); uptake factor $U \simeq 0.5$–1 (Bishop & Egil 2011; Feige et al. 2012) ➔ take either $fU = 0.06$ (cf. Knie et al. 2004) or 0.05 (lower limit)
4. Obtain number density of ^{60}Fe for each crust layer by summing Σ(t) within the corresponding time intervals and dividing it through the thickness of the layer
5. Relate n_{60Fe} to the density of stable iron (i.e., ^{60}Fe/Fe), given by $n_{Fe} = \frac{x_{Fe}\rho_{crust}N_A}{A_{Fe}} = 2.47 \times 10^{21}\ \mathrm{cm}^{-3}$

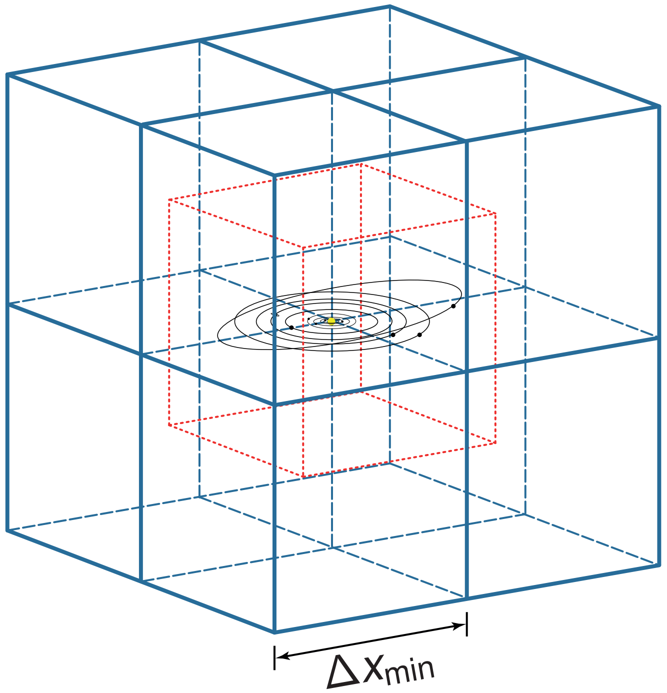

Evolution of the gas column density distribution (cuts through $z = 0$ and $y = 0$)

Model A (~ WIM)

$n = 0.1$ cm^{-3}

$T = 10^4$ K

$Z/Z_\odot = 1$

$\Delta x = 0.7$ pc

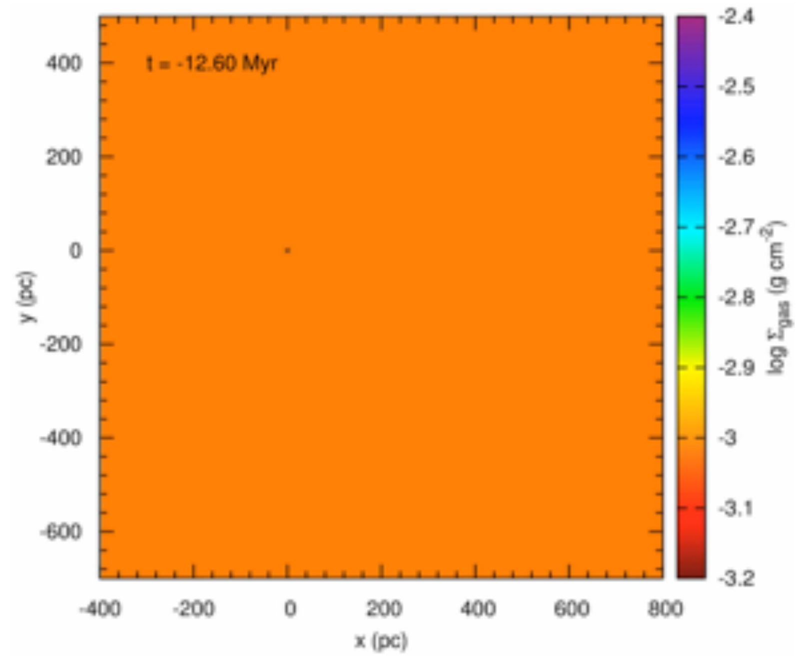

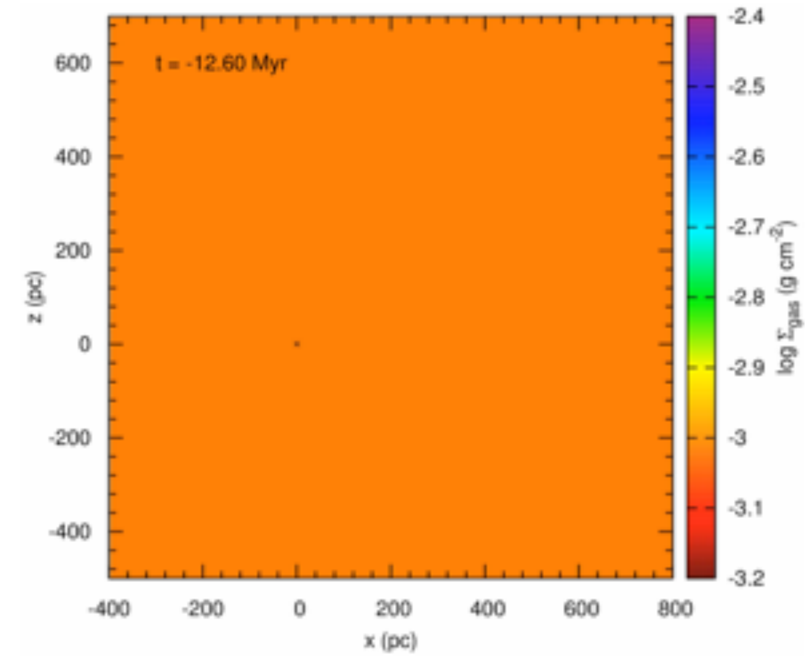

Model B (~ WNM)

$n = 0.3$ cm^{-3}

$T = 6800$ K

$Z/Z_\odot = 1$

$\Delta x = 0.7$ pc

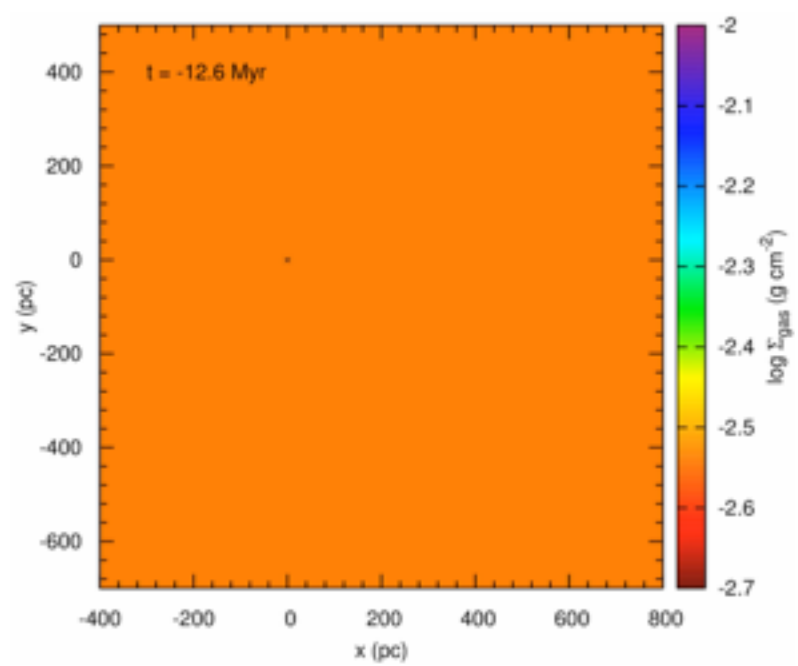

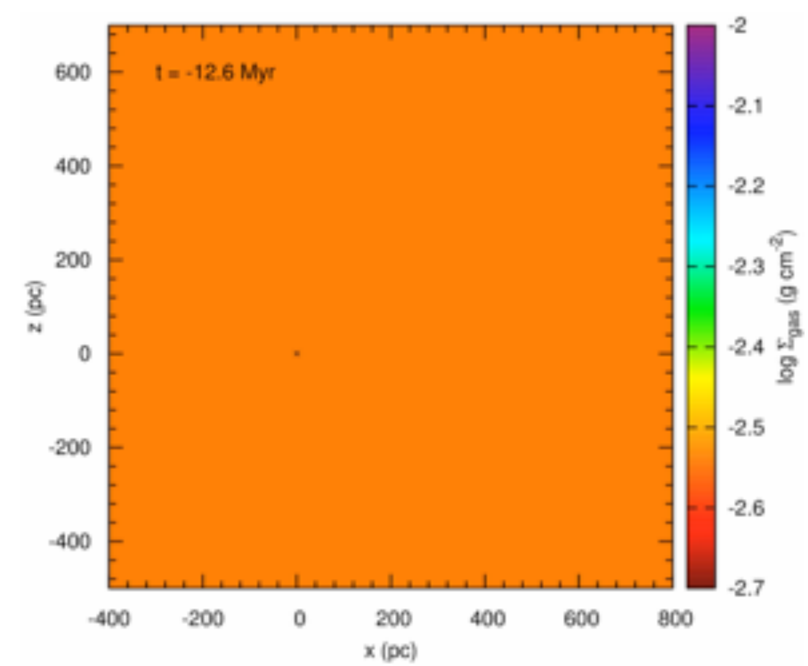

Results — Chemical mixing simulations with homogeneous background medium

Volume rendering of the present-day density distribution

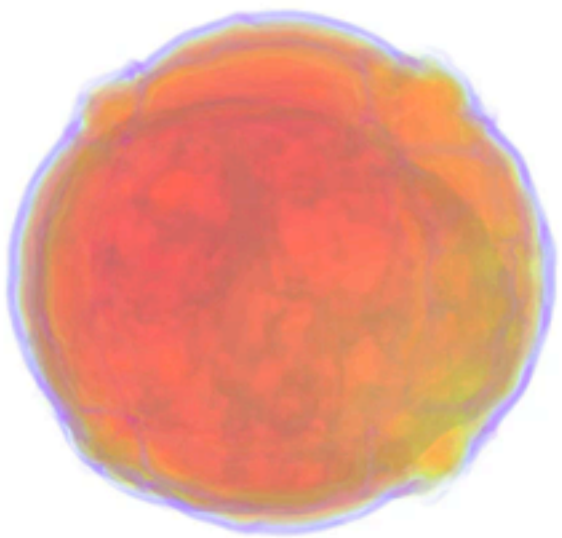

Model A

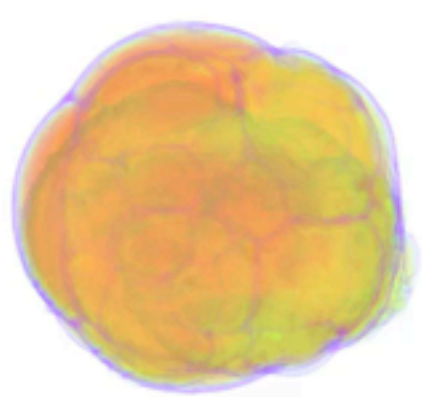

Model B

- LB and Loop I form almost coevally
- **At first:** independent evolution; thermal and fluid-dynamical instabilities occur ➔ formation of cold, dense clumps
  - Supershell accelerates (after SN): Rayleigh-Taylor instability (RTI) develops at contact discontinuity (most affected are parts of supershell that lie closest to SN explosion center ➔ inward growing filaments of dense gas ➔ mixing with hot bubble gas
  - Supershell decelerates (reduced or no SN activity): Vishniac over-stability at supershell surface due to mismatch between thermal and ram pressure ➔ growing, oscillating ripples
- **Later on:** shells collide after 3.0 (model A) and 4.6 Myr (model B)
  - Interaction layer that becomes RT unstable due to unequal pressure in SB cavities
  - Formation of cold, dense cloudlets that travel into less pressurized SB (LB)
- Shells break-up after 6.5 Myr (model A) or never (model B)
- 'Present' LB extension: (x,y,z) = (800,600,760) pc in model A; (580,480,540) pc in model B
- Hydrogen density and temperature in 'present' LB cavity: $10^{-4.2}$–$10^{-3.9}$ cm^{-3}, $10^{6.9}$–$10^{7.1}$ K in model A; $10^{-4.2}$–10^{-3} cm^{-3}, $10^{5.8}$–10^{7} K in model B
- Poor matching between calculated and observed extensions due to absence of neighbouring clouds and vertical gradients ➔ solar system might 'shift' closer to LB center
- Exact extensions not crucial for ^{60}Fe transport modeling during the time the solar system resides within the LB (except for supershell arrival!)

Results — Chemical mixing simulations with homogeneous background medium

Evolution of the ^{60}Fe mass density distribution (cuts through $z = 0$ and $y = 0$)

Model A (~ WIM)

$n = 0.1$ cm^{-3}

$T = 10^4$ K

$Z/Z_\odot = 1$

$\Delta x = 0.7$ pc

Model B (~ WNM)

$n = 0.3$ cm^{-3}

$T = 6800$ K

$Z/Z_\odot = 1$

$\Delta x = 0.7$ pc

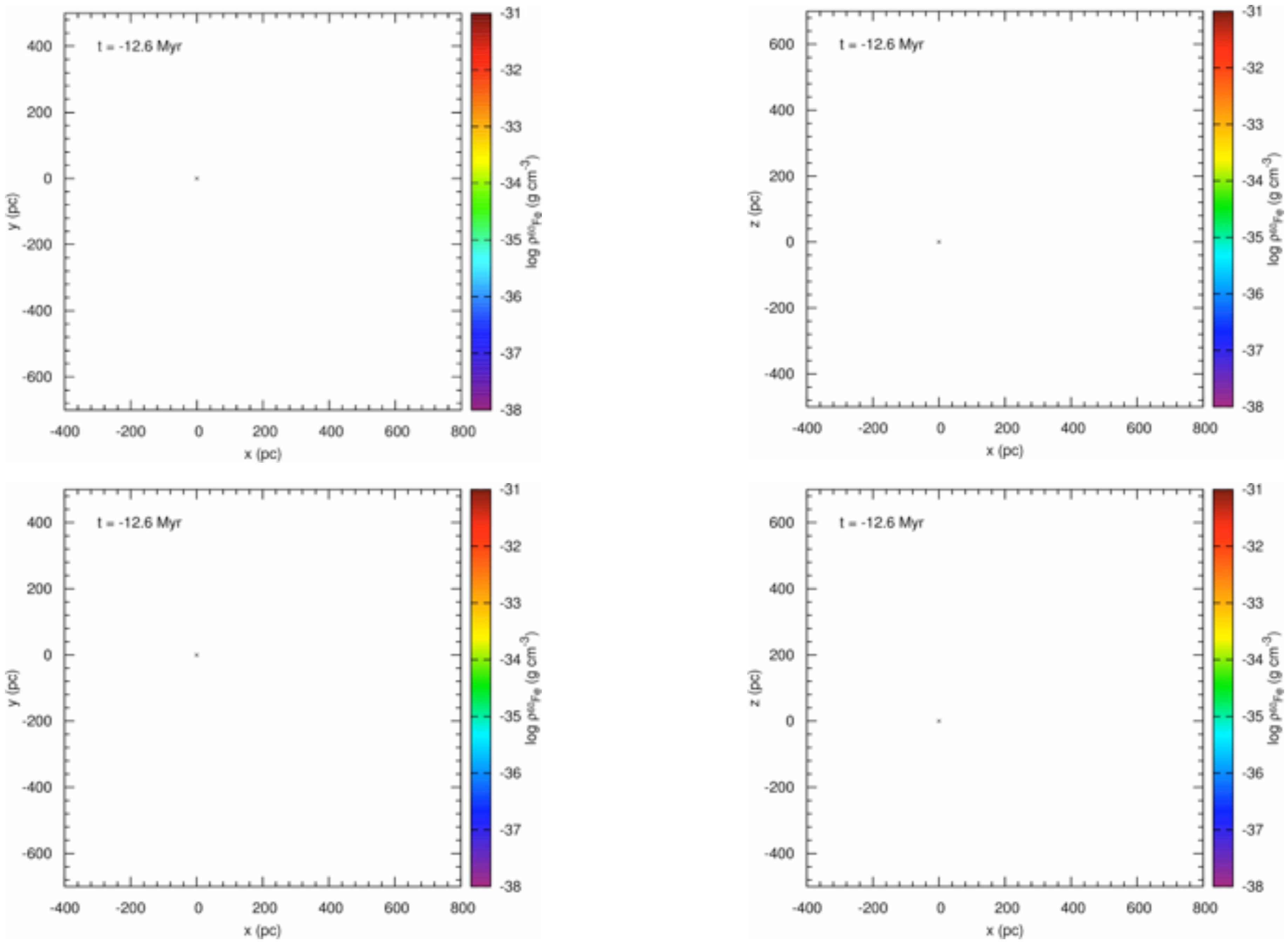

- Inhomogeneities arising from recent SNe are smoothed out over time due to turbulent shear flows inside the SB cavities
- Injection of turbulence by SNRs running into supershell and generating asymmetric reflected shocks
- Time scale of mixing: $\tau_m \lesssim \ell/a$ = (100 pc)/(100 km s^{-1}) = 1 Myr
- ^{60}Fe very homogenized since last LB SN occurred about 1.5 Myr ago

Results — Chemical mixing simulations with homogeneous background medium

Model A: Entropy maps and temporal variation of the local interstellar fluence of ^{60}Fe atoms

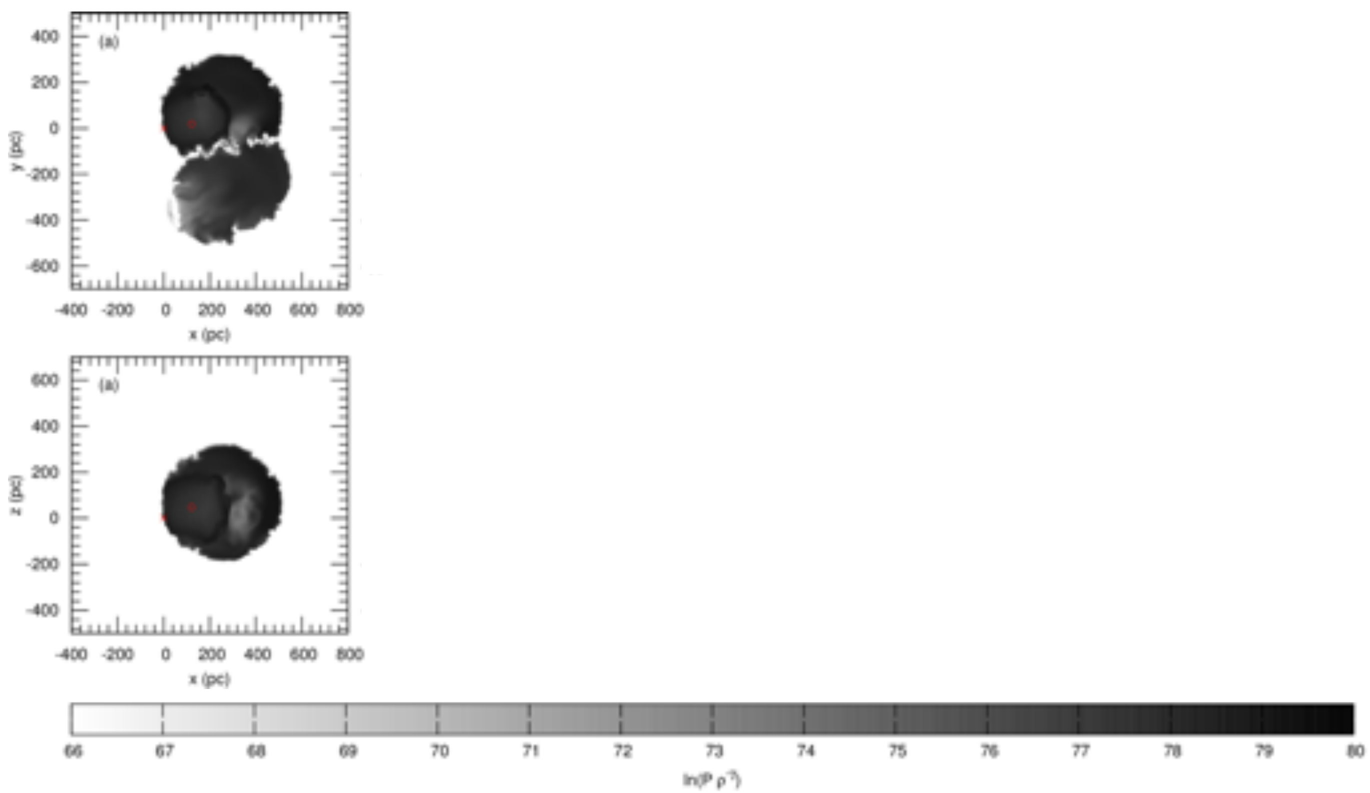

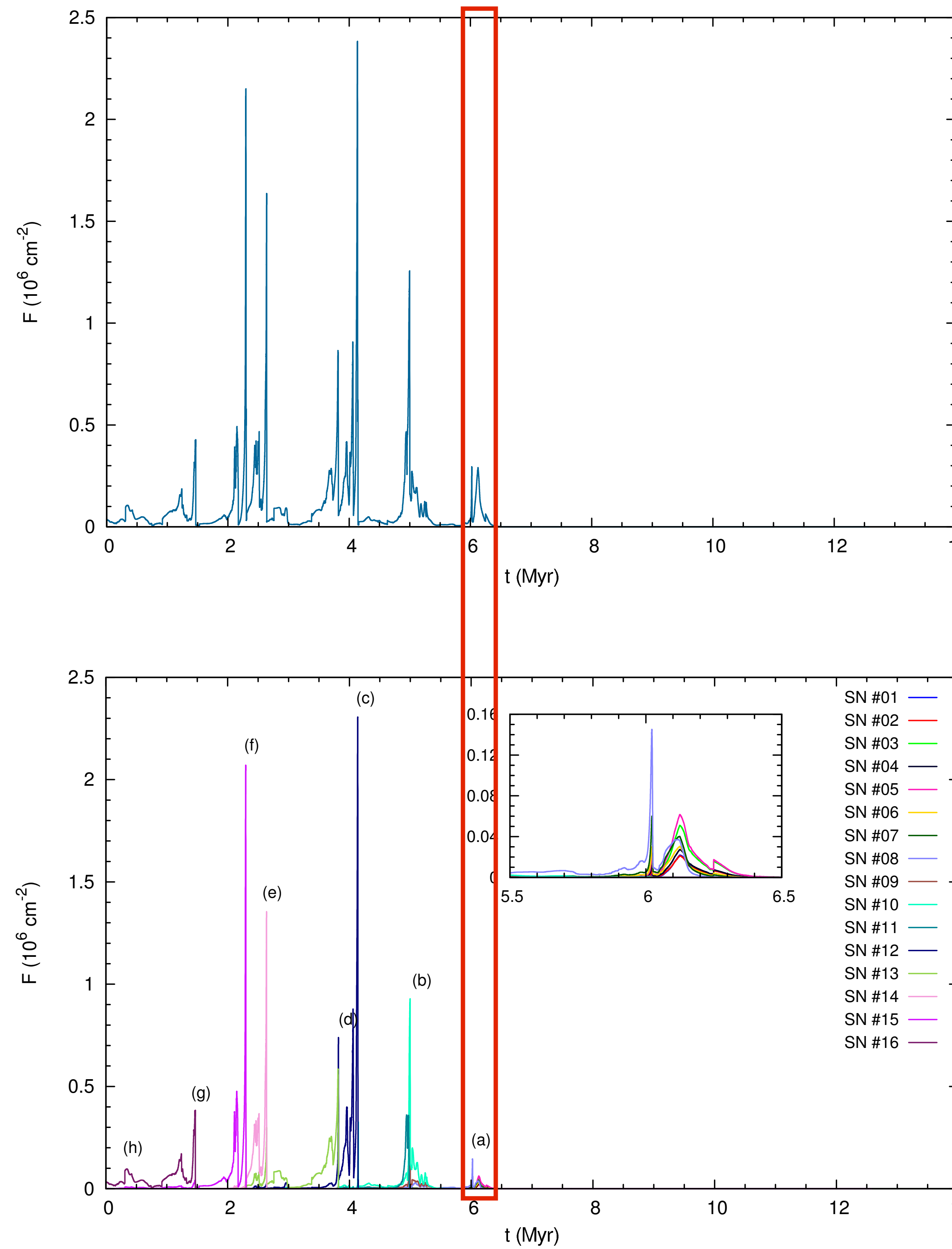

Results — Chemical mixing simulations with homogeneous background medium

Model A: Entropy maps and temporal variation of the local interstellar fluence of ^{60}Fe atoms

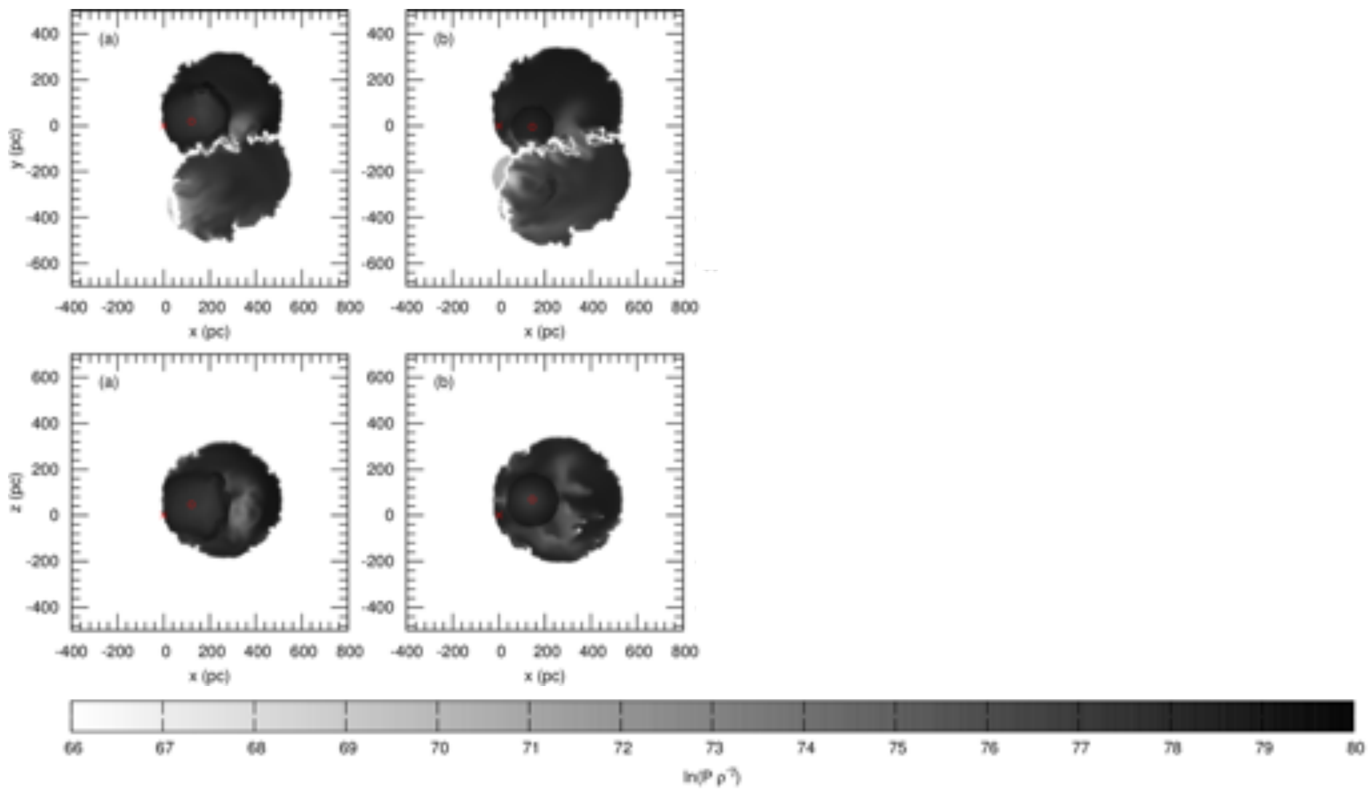

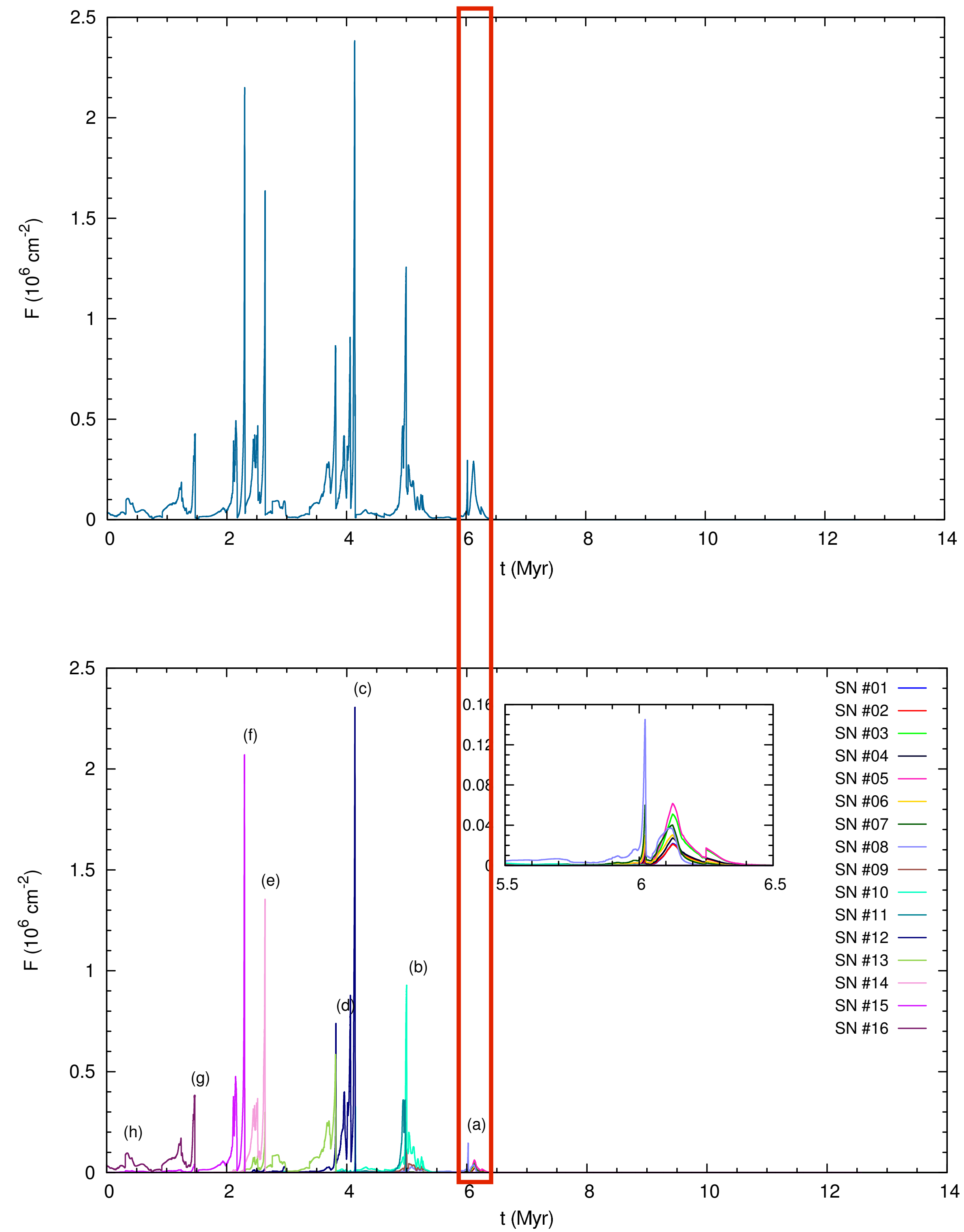

Results — Chemical mixing simulations with homogeneous background medium

Model A: Entropy maps and temporal variation of the local interstellar fluence of ^{60}Fe atoms

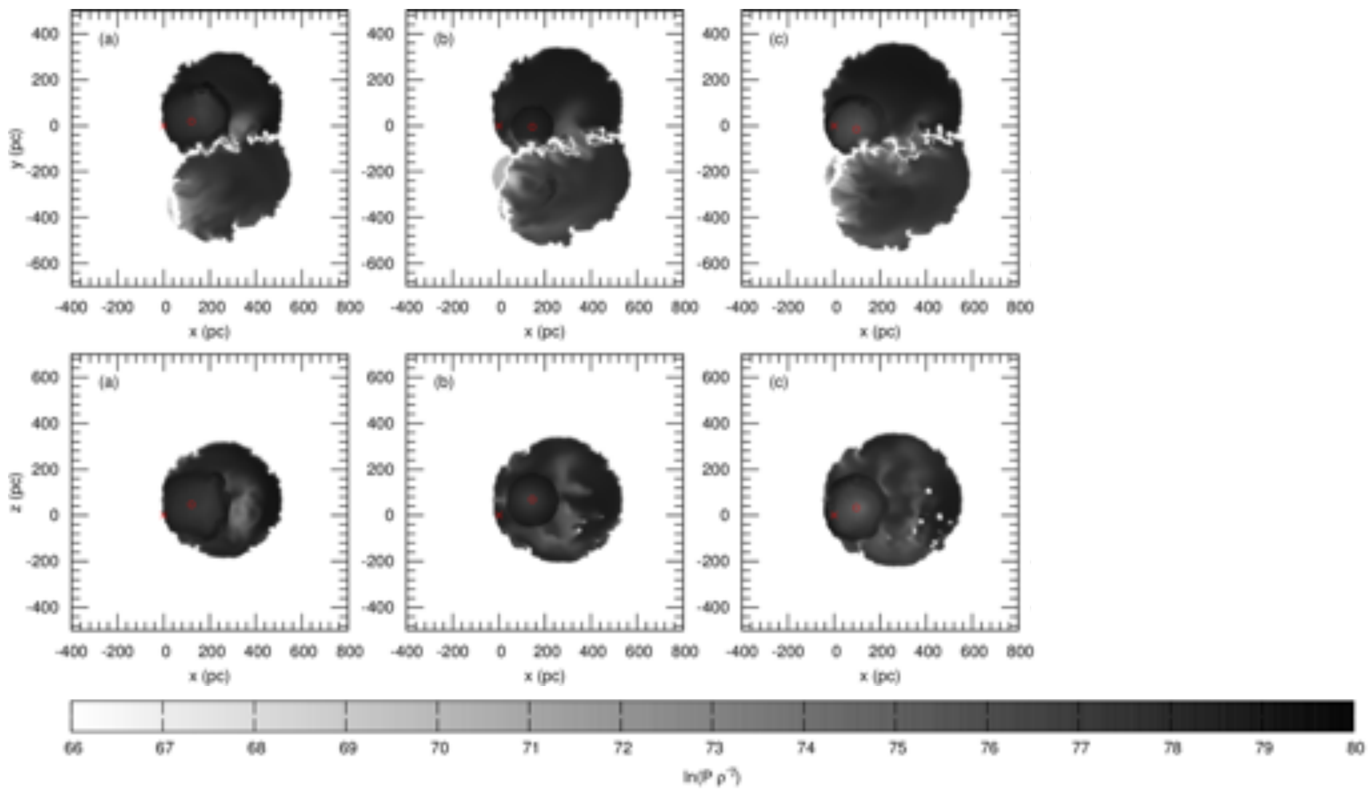

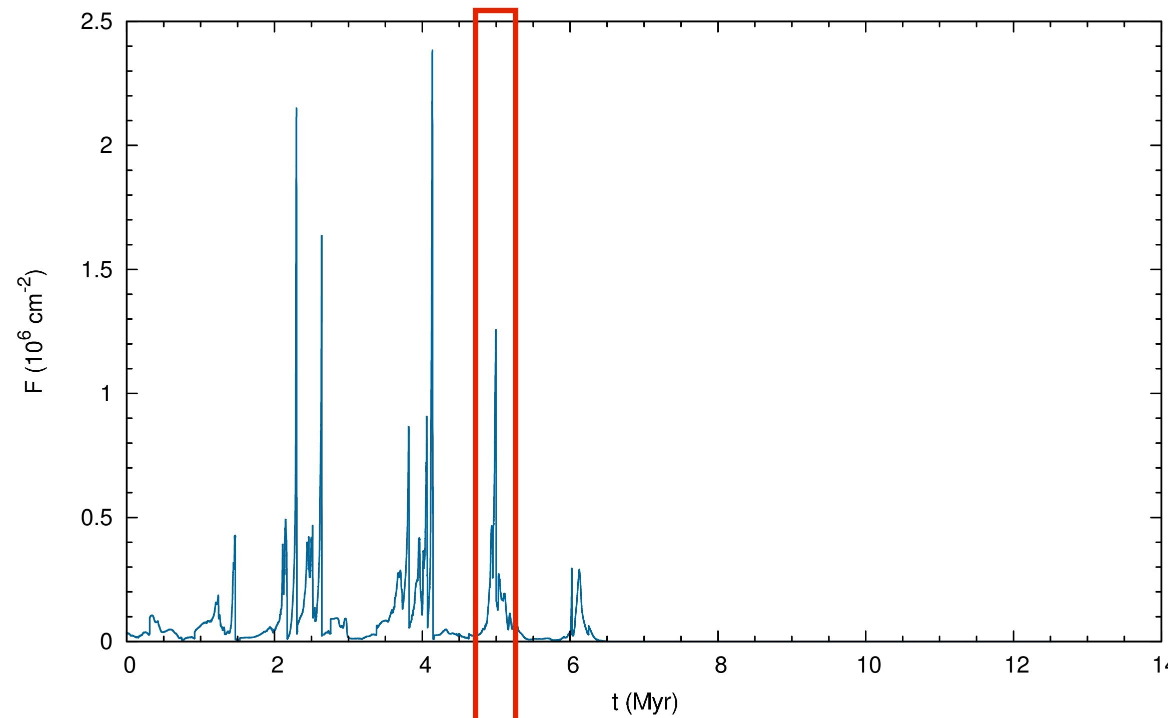

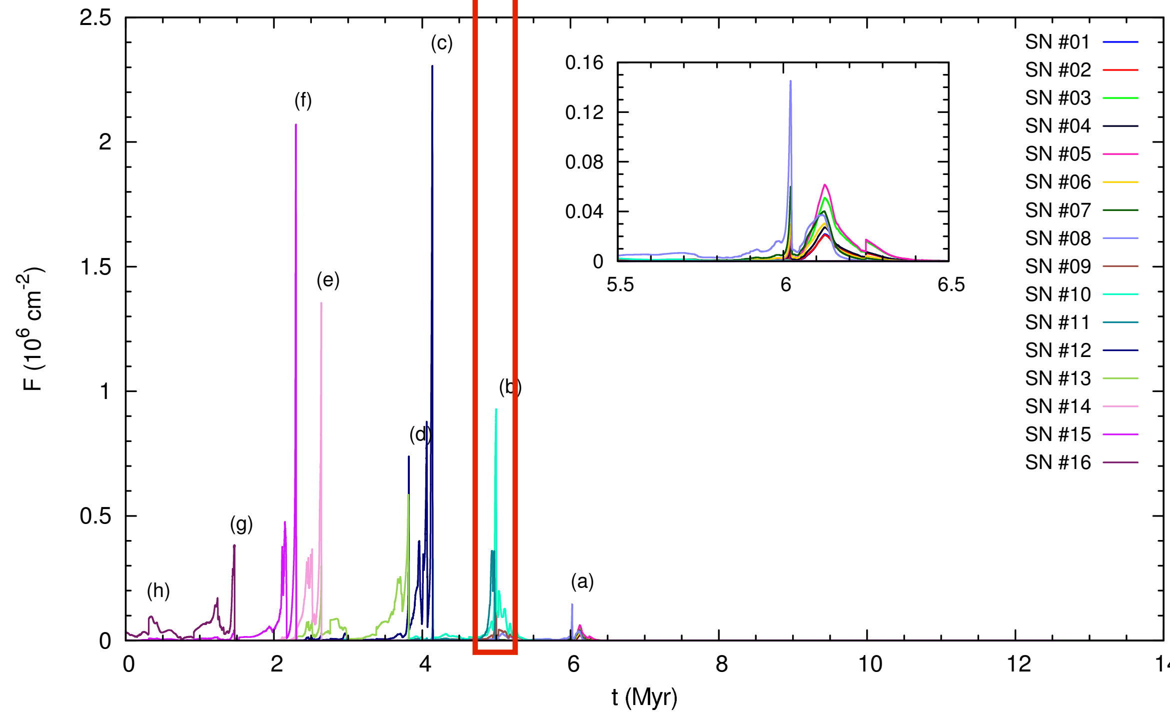

Results — Chemical mixing simulations with homogeneous background medium

Model A: Entropy maps and temporal variation of the local interstellar fluence of ^{60}Fe atoms

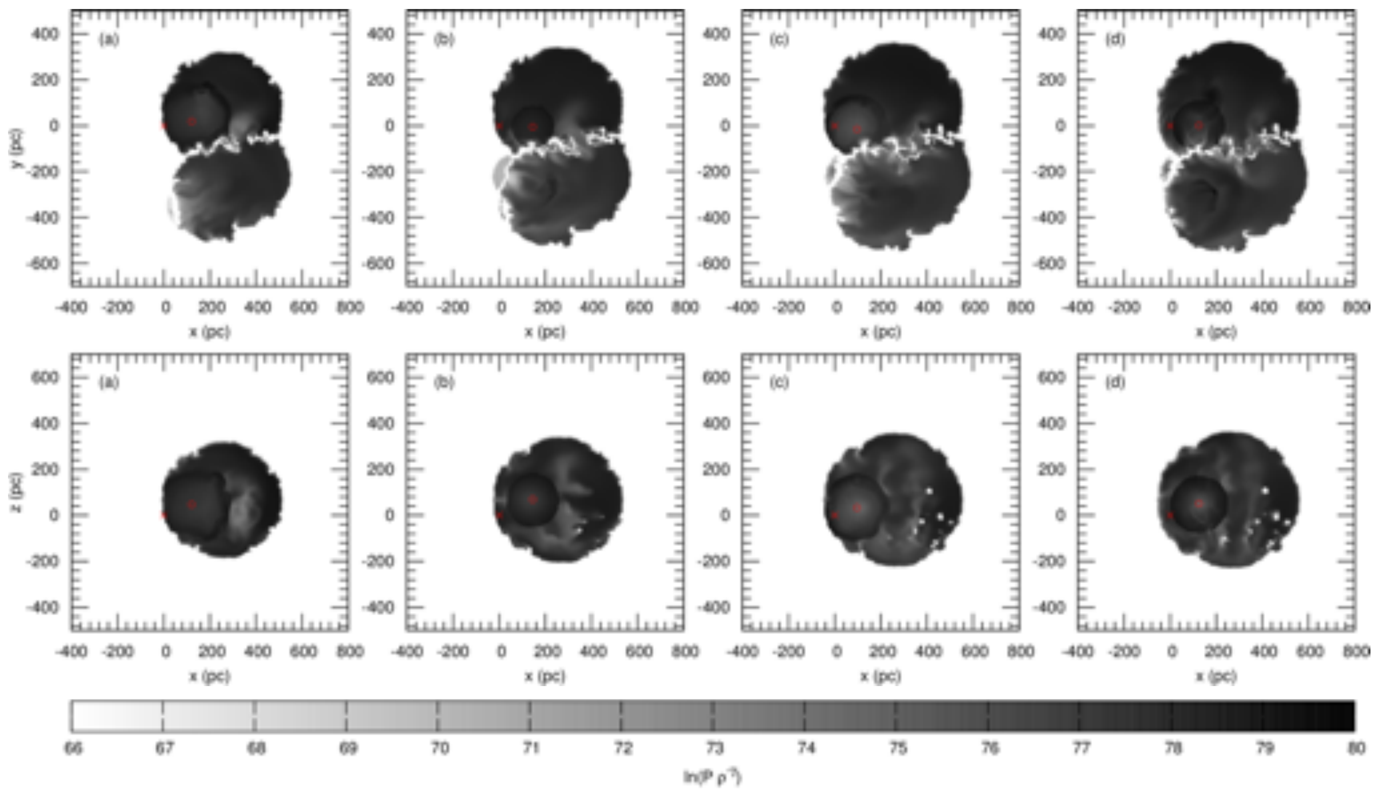

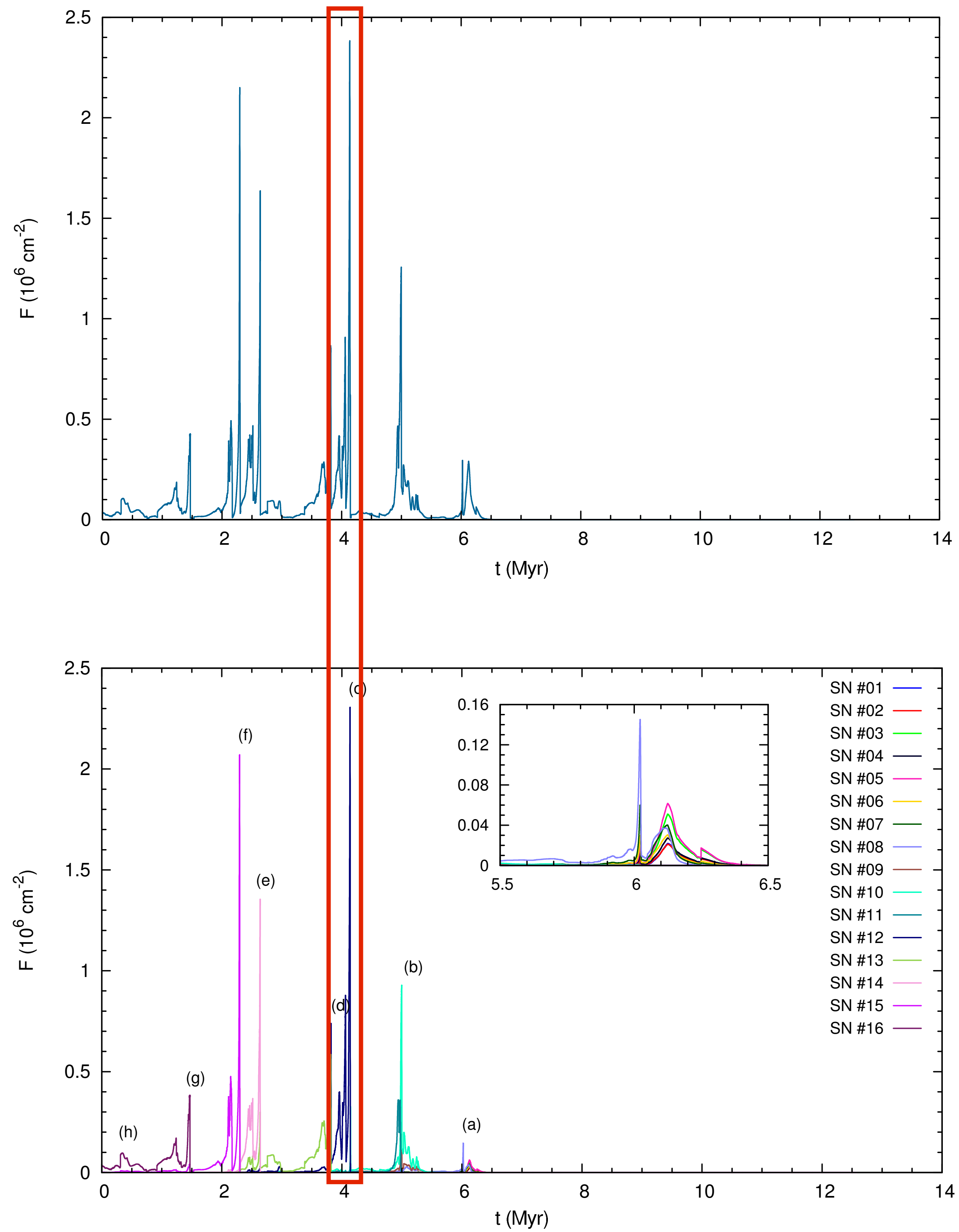

Results — Chemical mixing simulations with homogeneous background medium

Model A: Entropy maps and temporal variation of the local interstellar fluence of ^{60}Fe atoms

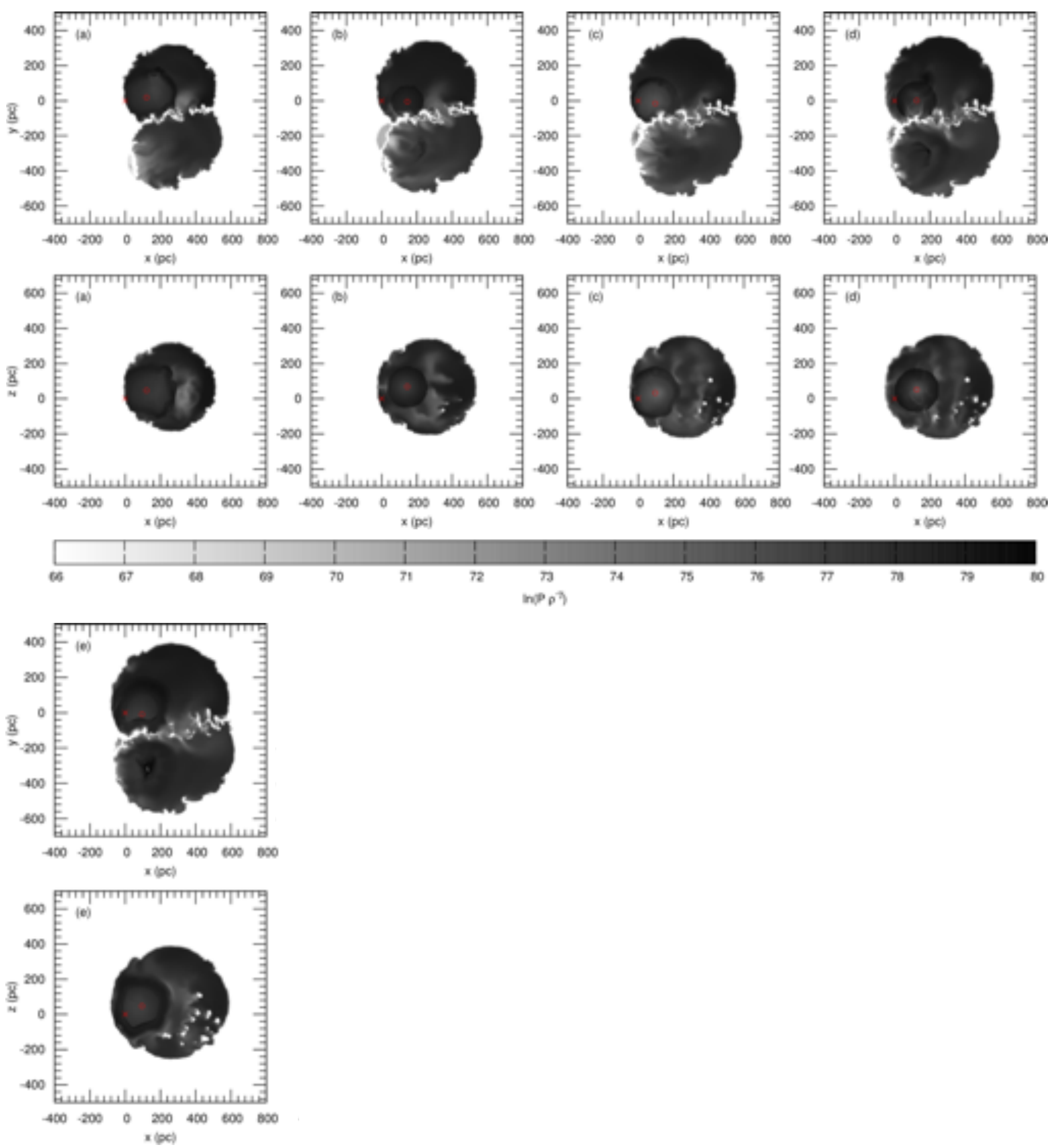

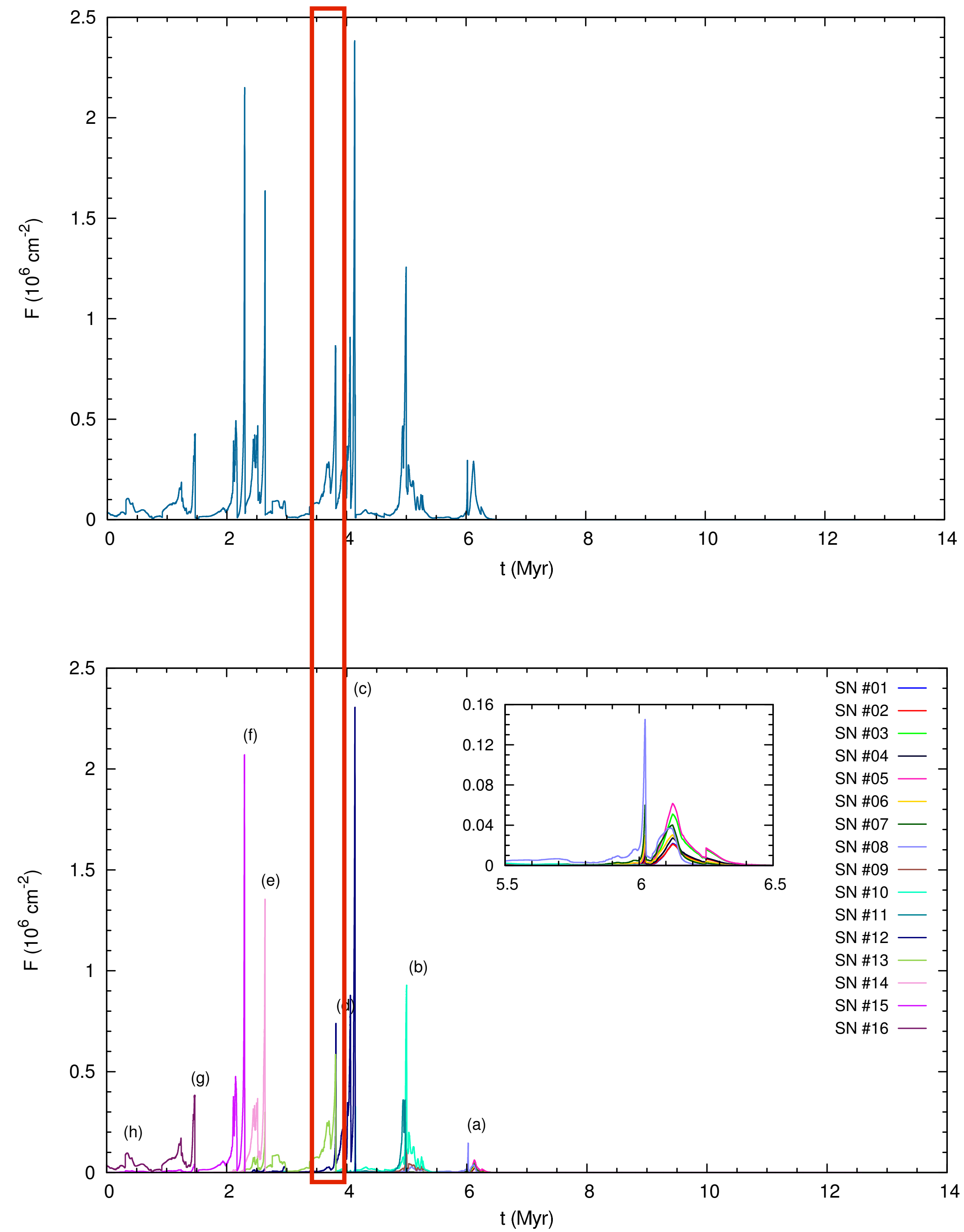

Results — Chemical mixing simulations with homogeneous background medium

Model A: Entropy maps and temporal variation of the local interstellar fluence of ^{60}Fe atoms

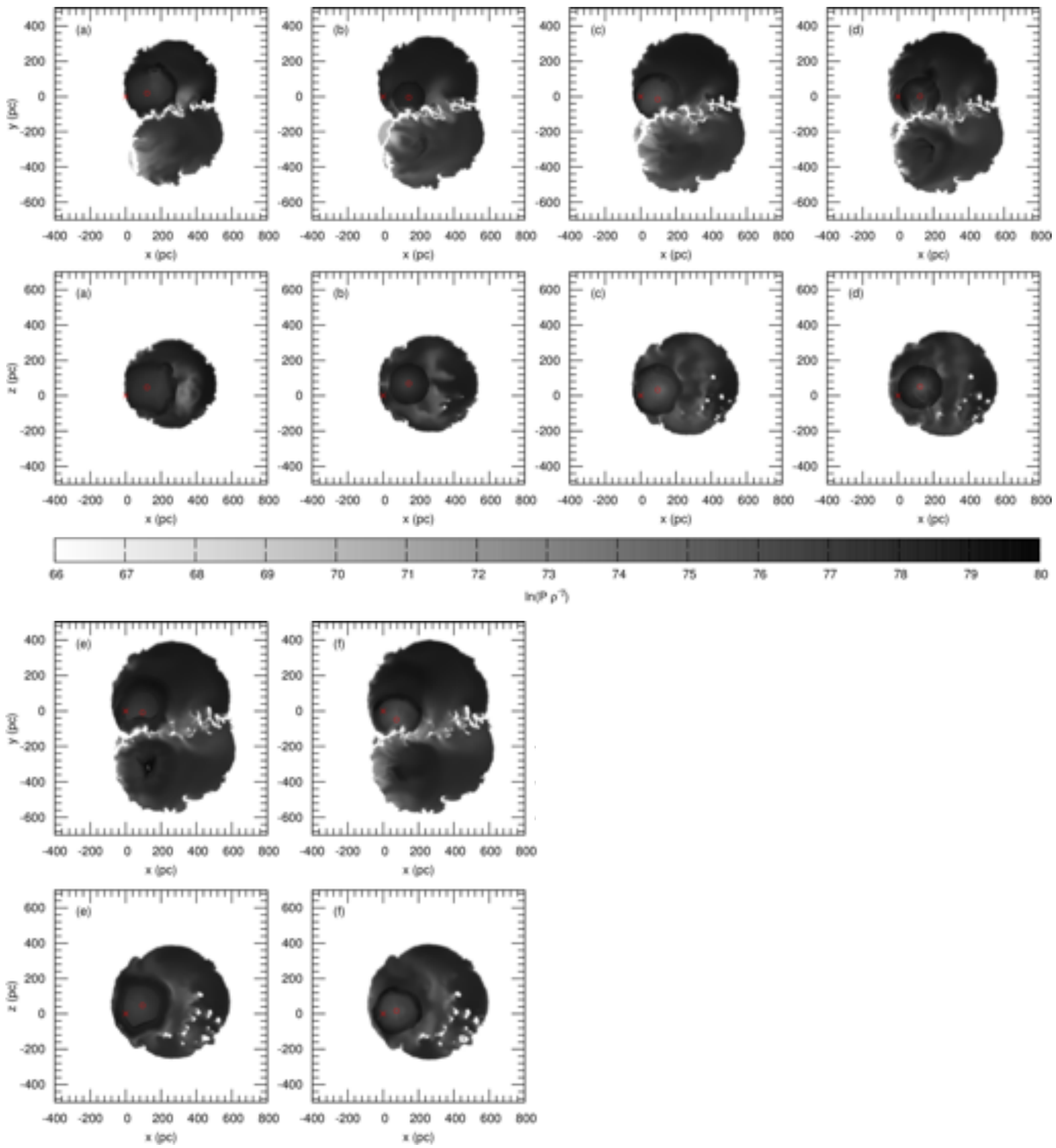

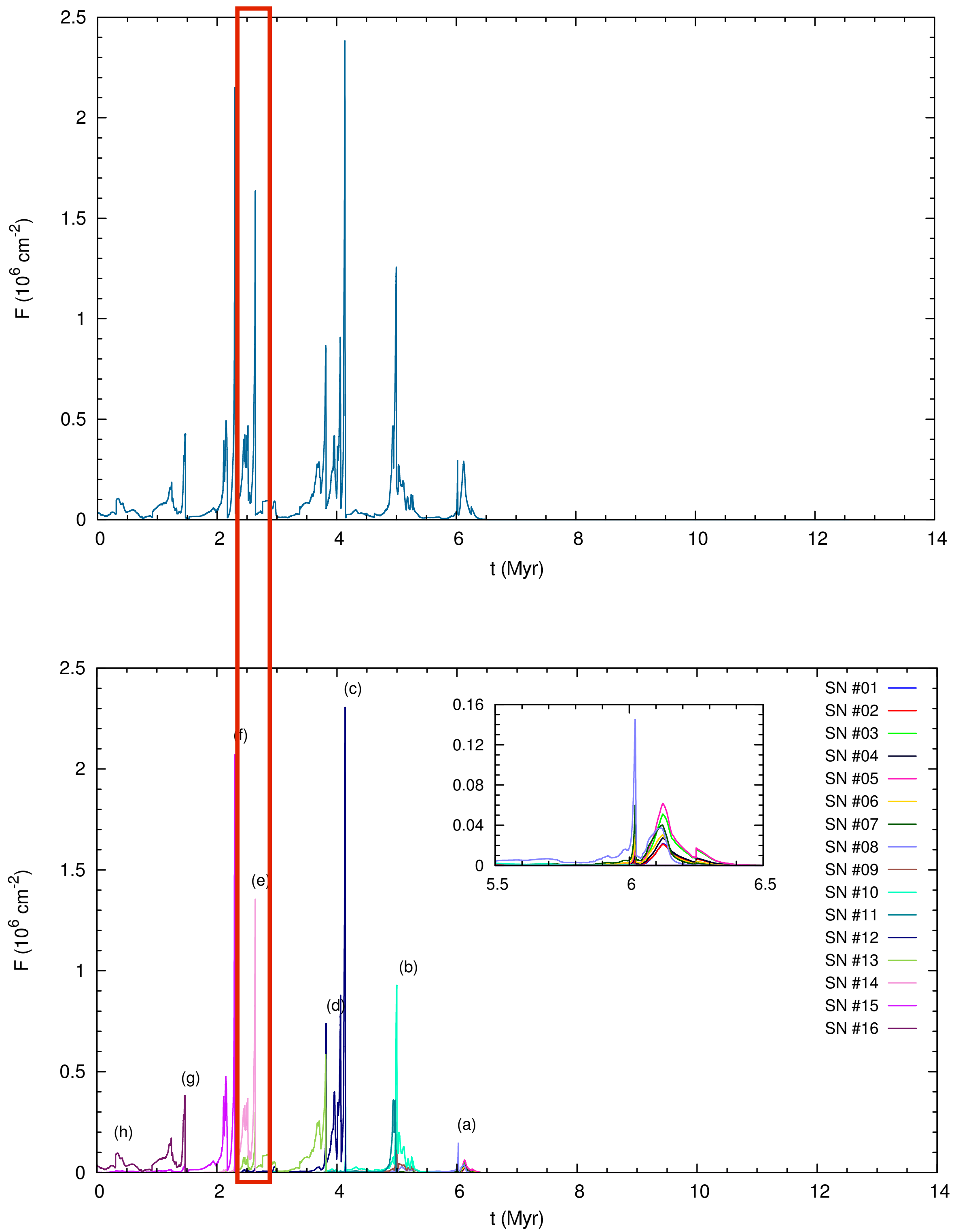

Results — Chemical mixing simulations with homogeneous background medium

Model A: Entropy maps and temporal variation of the local interstellar fluence of ^{60}Fe atoms

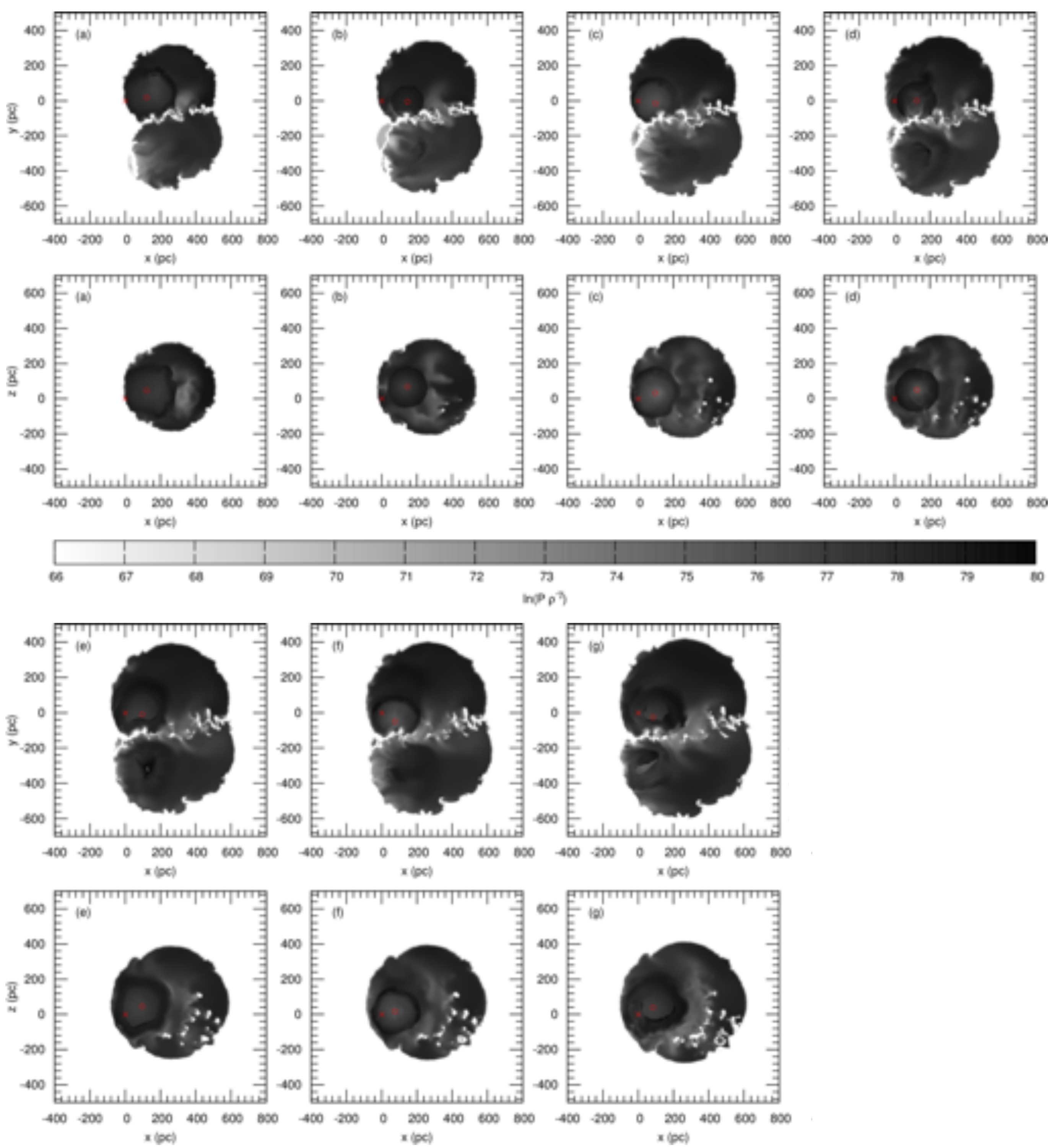

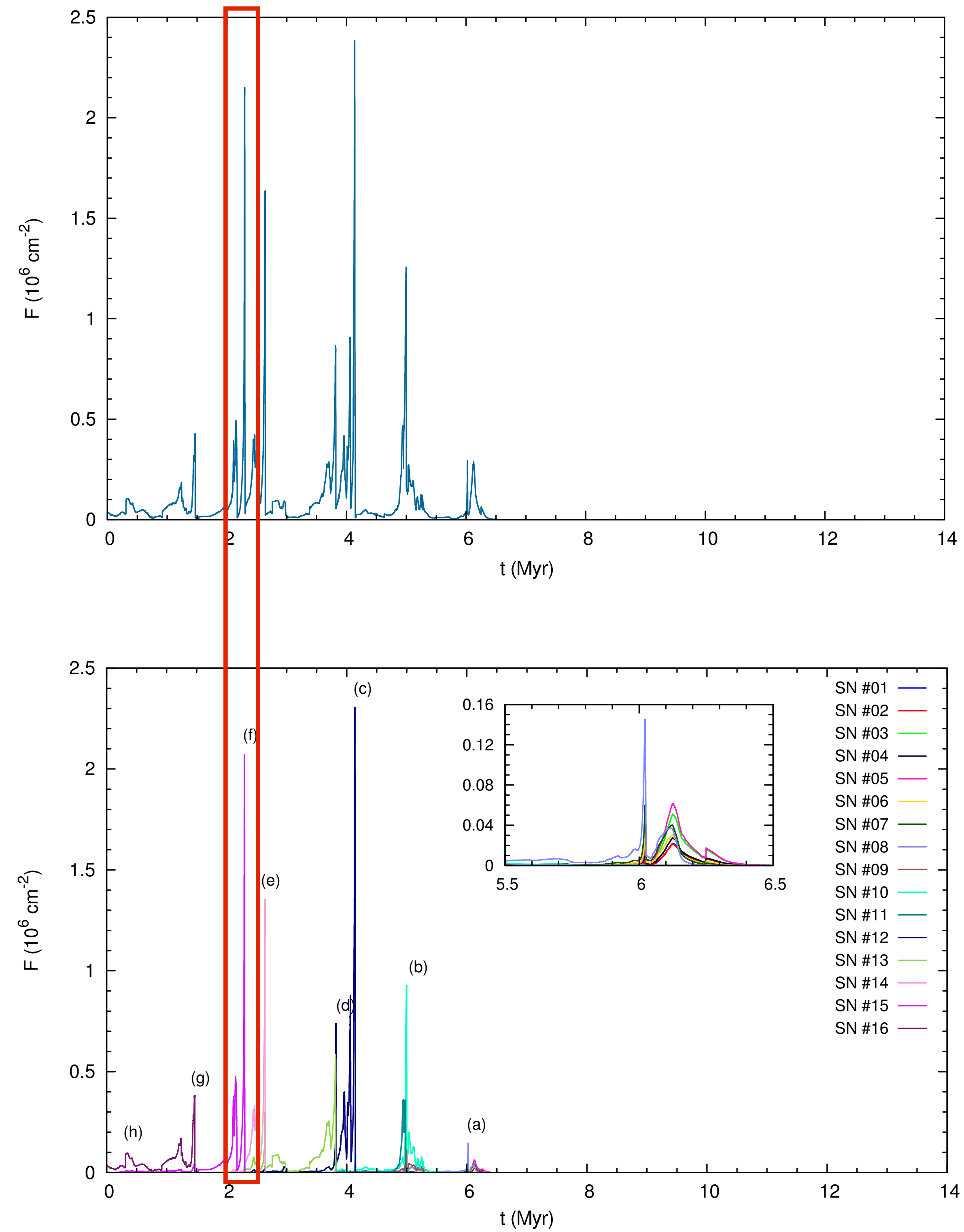

Results — Chemical mixing simulations with homogeneous background medium

Model A: Entropy maps and temporal variation of the local interstellar fluence of ^{60}Fe atoms

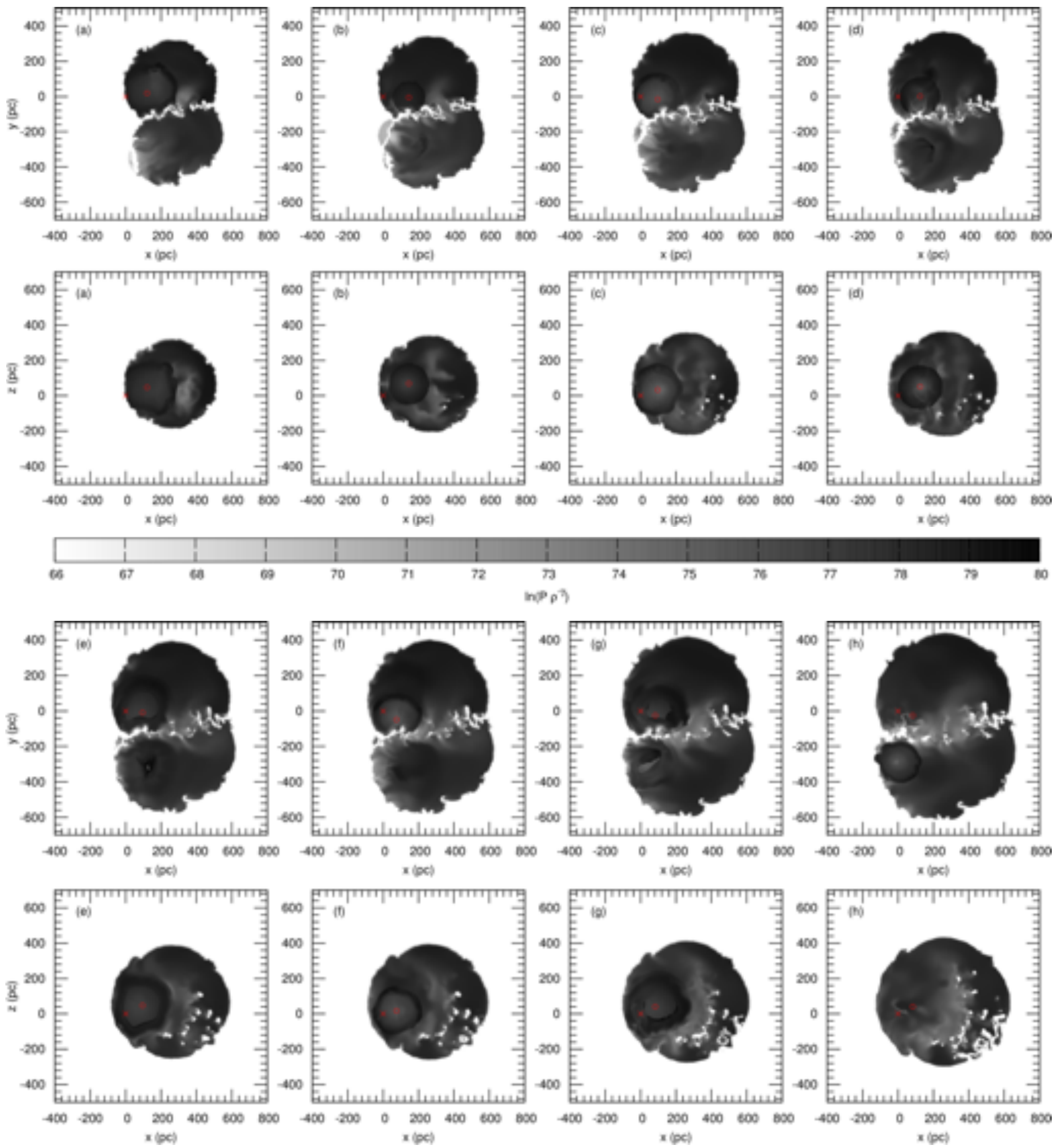

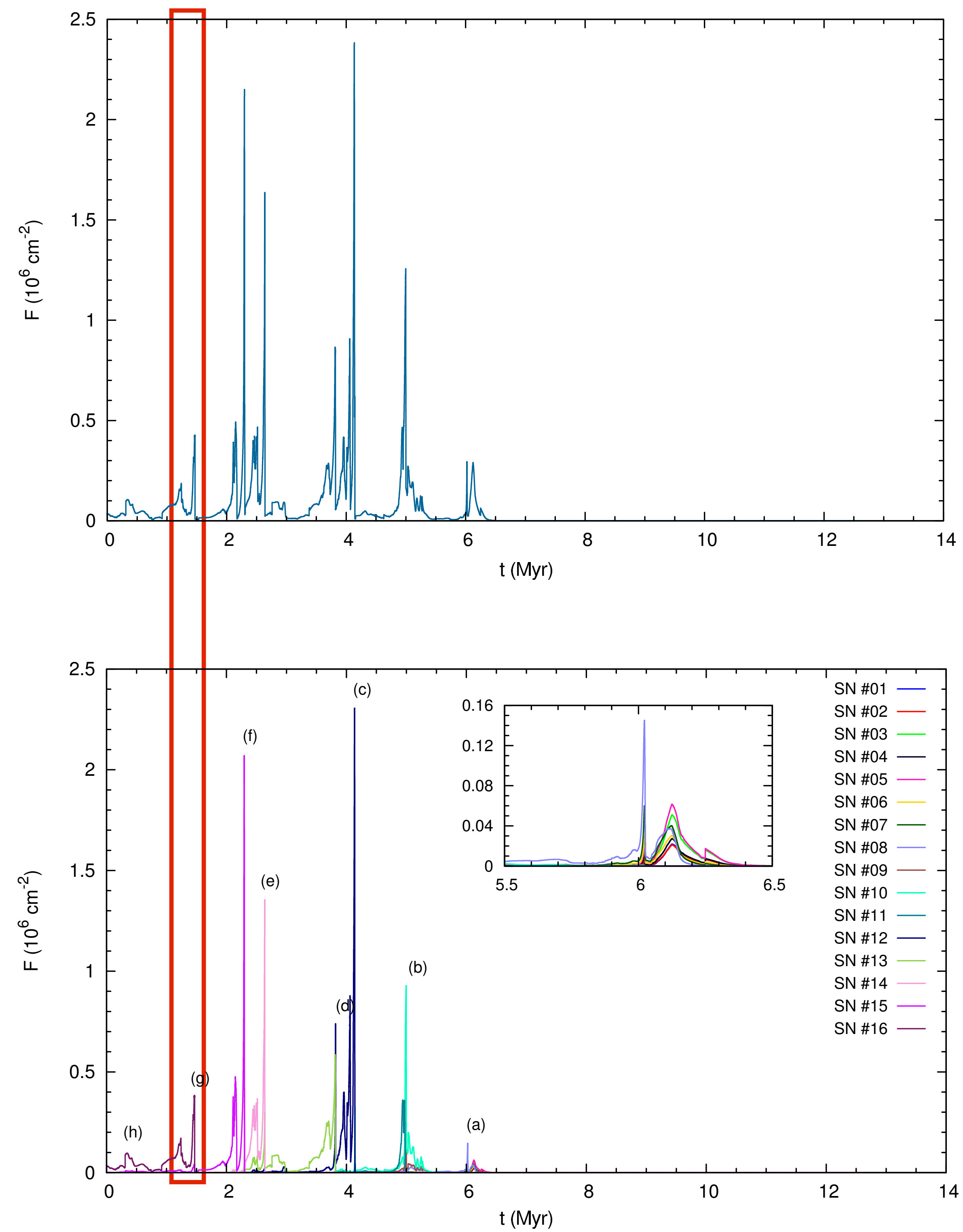

Results — Chemical mixing simulations with homogeneous background medium

Model A: Entropy maps and modeled $^{60}Fe/Fe$ content in the FeMn crust

- Three different types of signals embedded in ‘background noise’ with $\overline{F} \simeq 10^5$ cm^{-2} (turbulent motions in LB interior):
  1. High and sharp sawtooth waves due to Sedov-Taylor-phase SNRs (exposure time: $\Delta t \simeq$ 70-130 kyr ~ shell thickness; in agreement with literature)
  2. Weaker but more extended signals occurring (with increasing lag) after almost every sawtooth wave due to blast wave reflection from supershell (*SN ‘echoes’*)
  3. Broad signal at the beginning of the profile ($\Delta t \gtrsim$ 300 kyr) due to arrival of LB supershell
- All pulses entrain fractions of previously released ^{60}Fe that has not yet decayed
- ^{60}Fe should arrive on Earth as **dust**:
  - ‘Filtering’ due to partial condensation, loss during SNR expansion, collision between SNR and solar wind bubble
  - Remaining $f \simeq 1\%$ with grain sizes $\lesssim 0.2\ \mu$m (Fry et al. 2015) travel almost ballistically through solar system
  - If combined with newly-derived uptake factor, U = 0.5-1 (Bishop & Egli 2011; Feige et al. 2012) ➔ lower limit of combined factor: $fU \simeq 0.005$

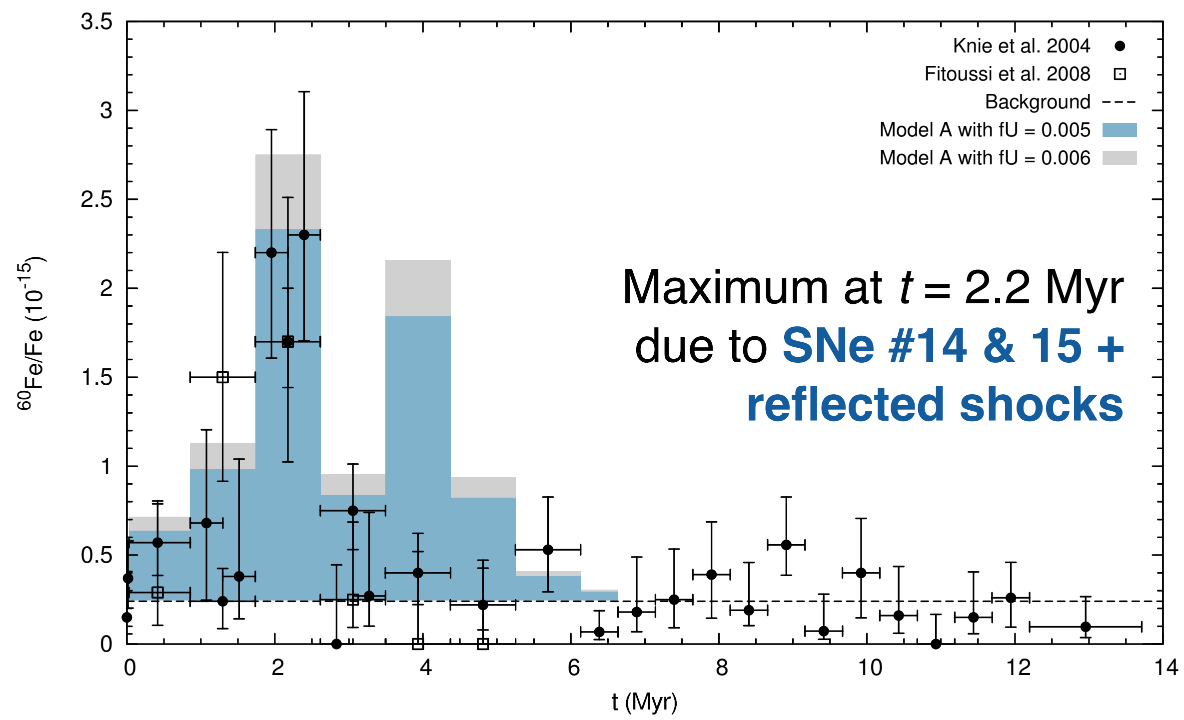

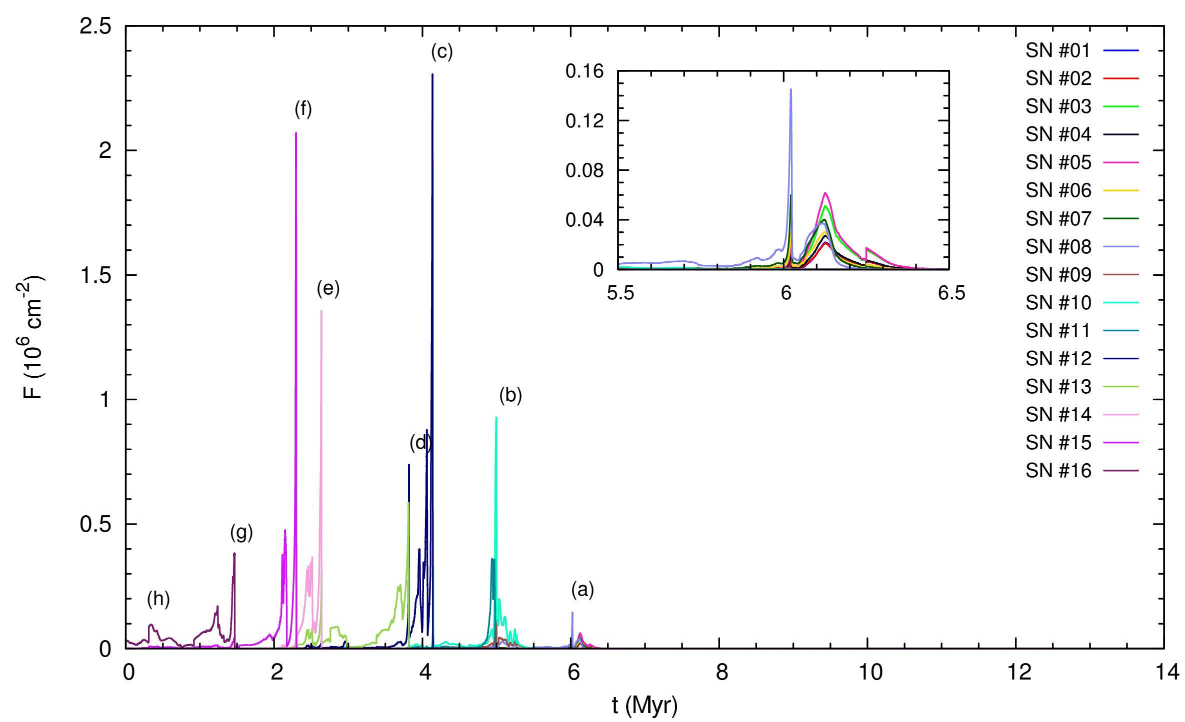

Results — Chemical mixing simulations with homogeneous background medium

Model B: Entropy maps and temporal variation of the local interstellar fluence of ^{60}Fe atoms

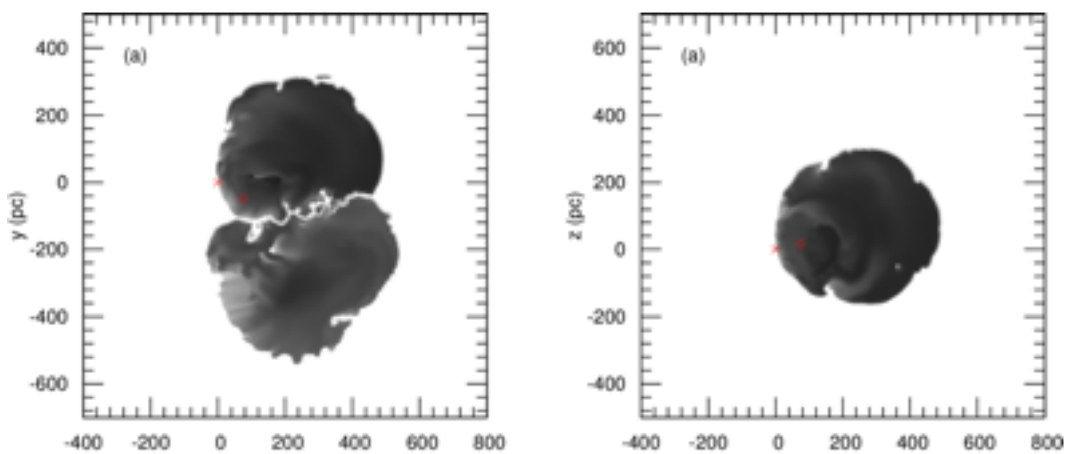

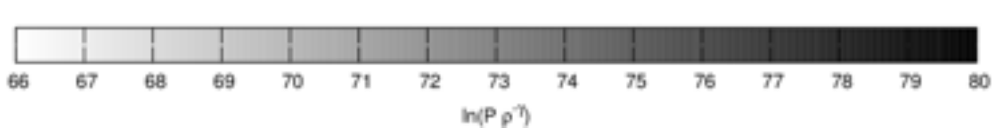

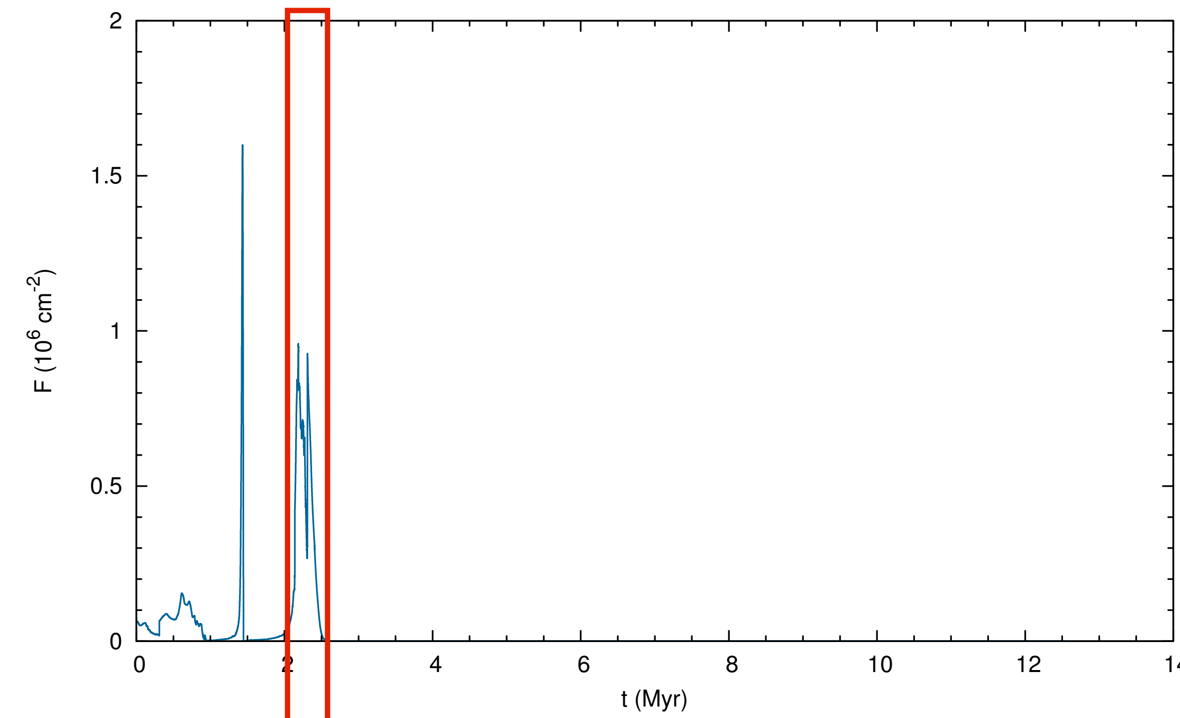

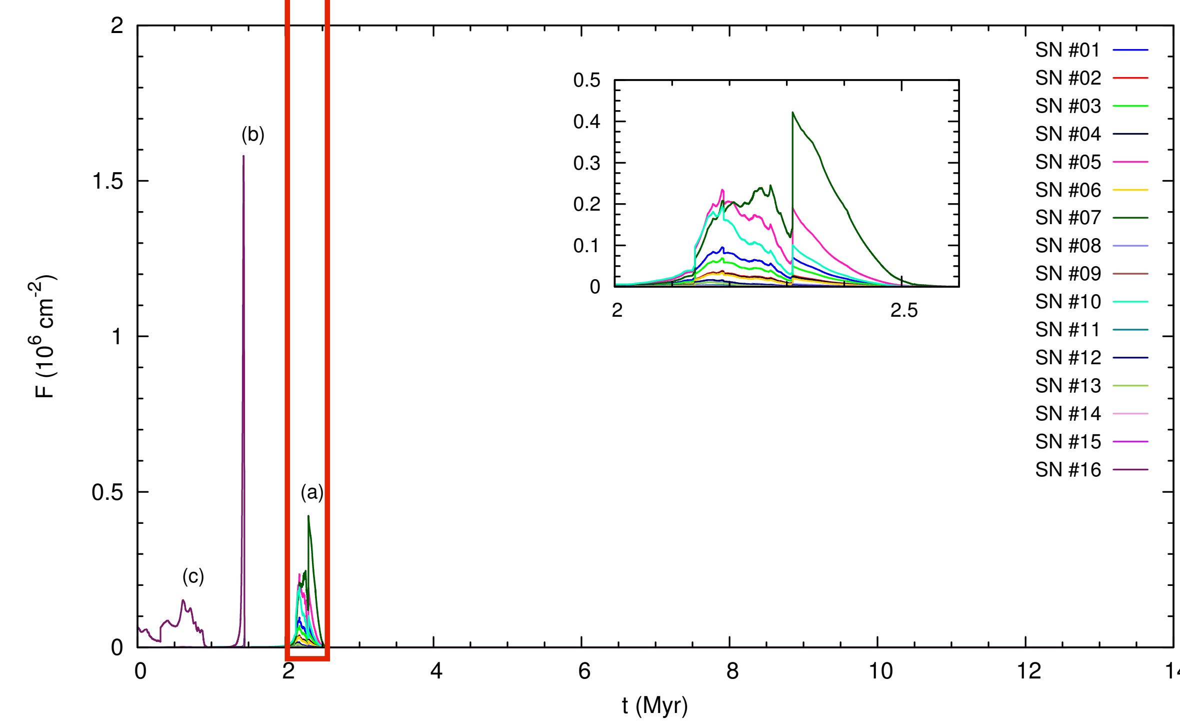

Results — Chemical mixing simulations with homogeneous background medium

Model B: Entropy maps and temporal variation of the local interstellar fluence of ^{60}Fe atoms

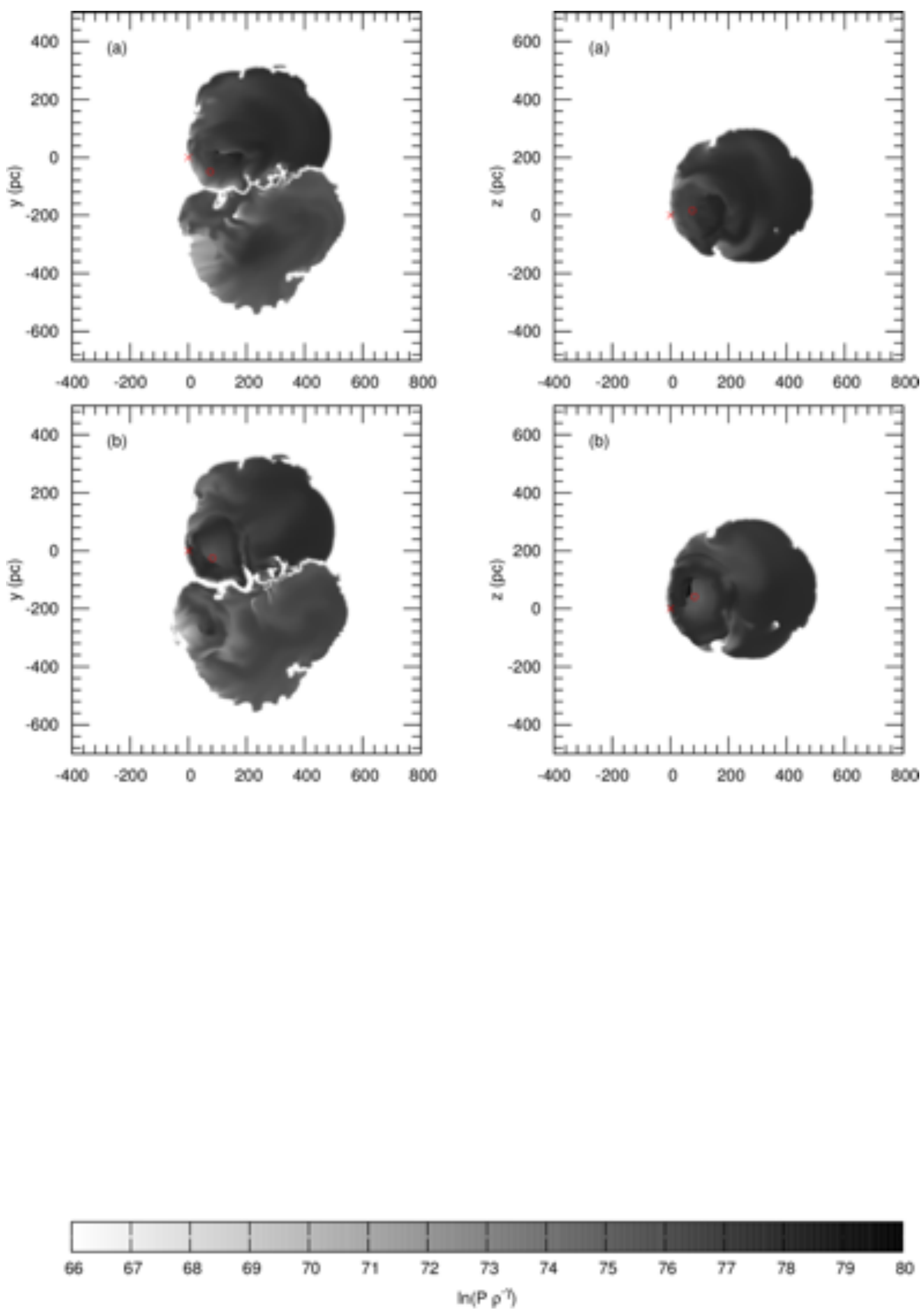

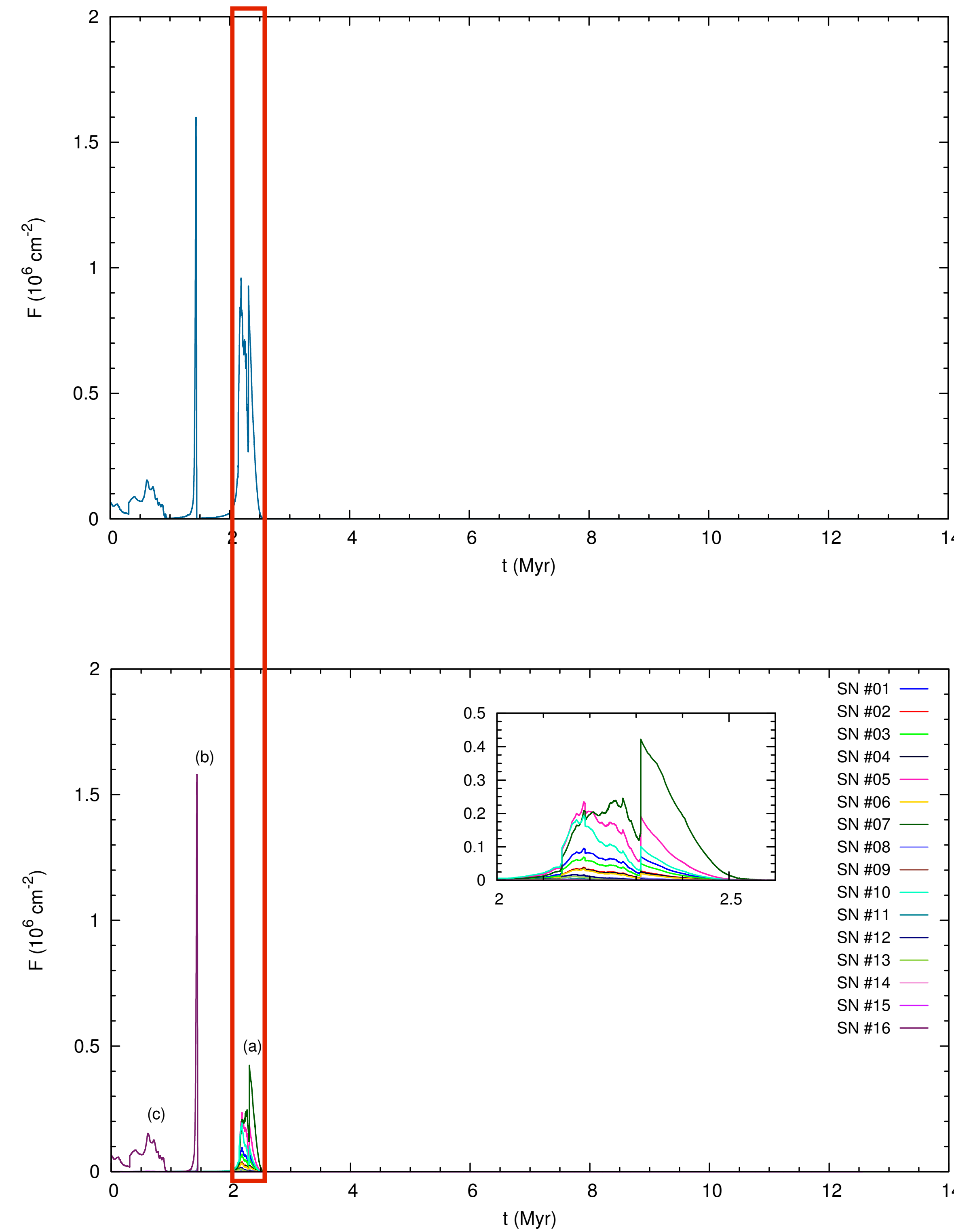

Results — Chemical mixing simulations with homogeneous background medium

Model B: Entropy maps and temporal variation of the local interstellar fluence of ^{60}Fe atoms

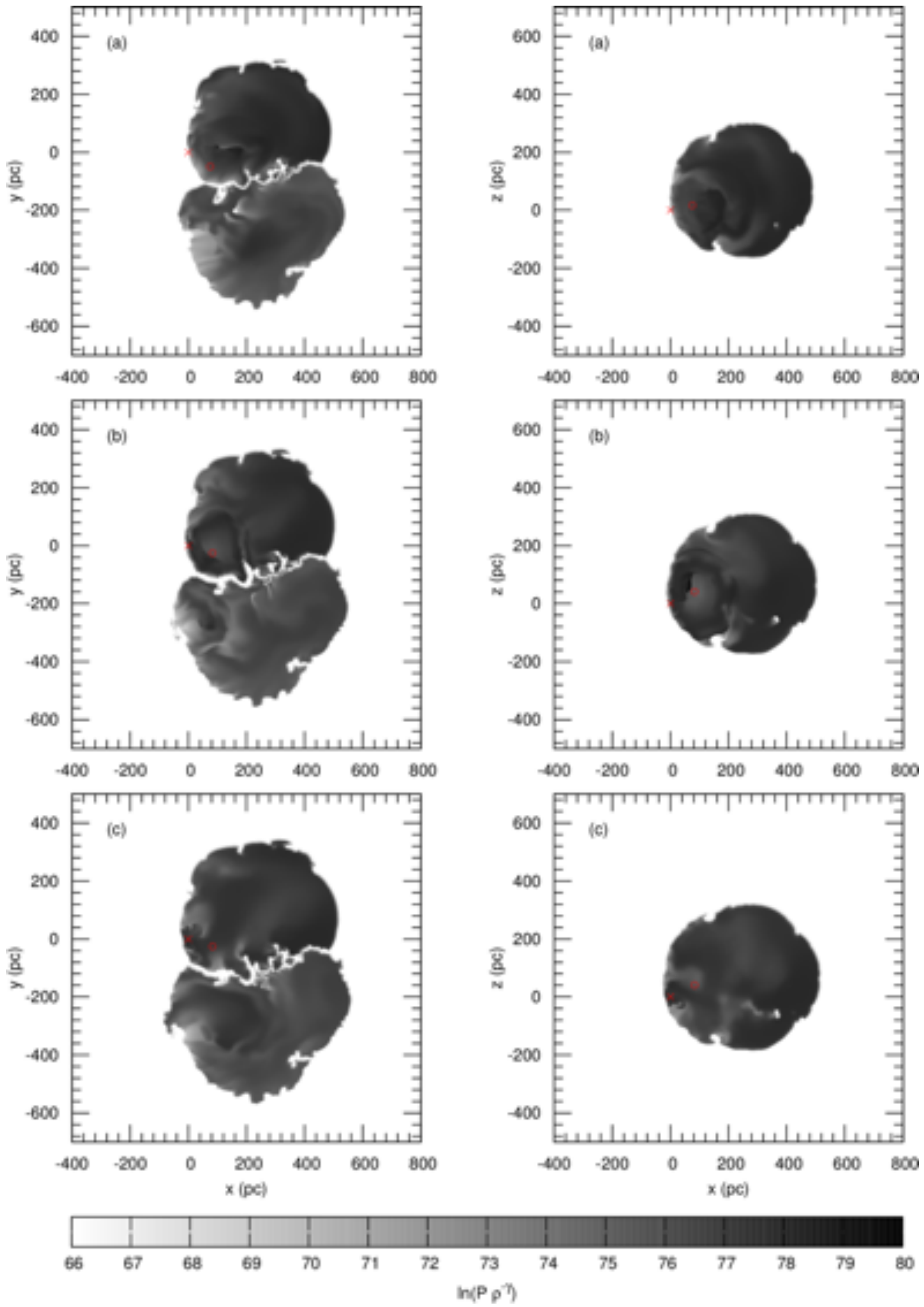

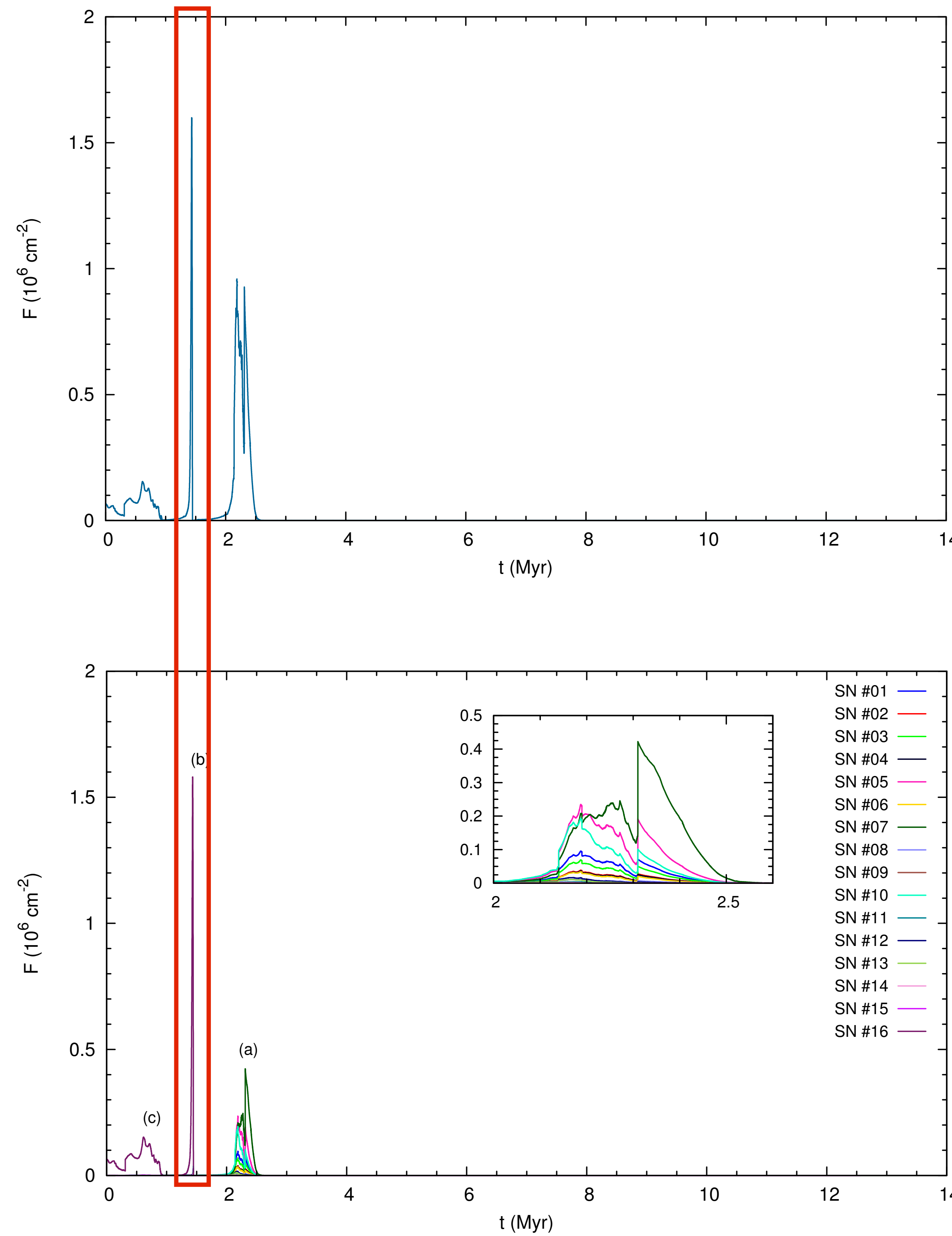

Results — Chemical mixing simulations with homogeneous background medium

Model B: Entropy maps and modeled ^{60}Fe/Fe content in the FeMn crust

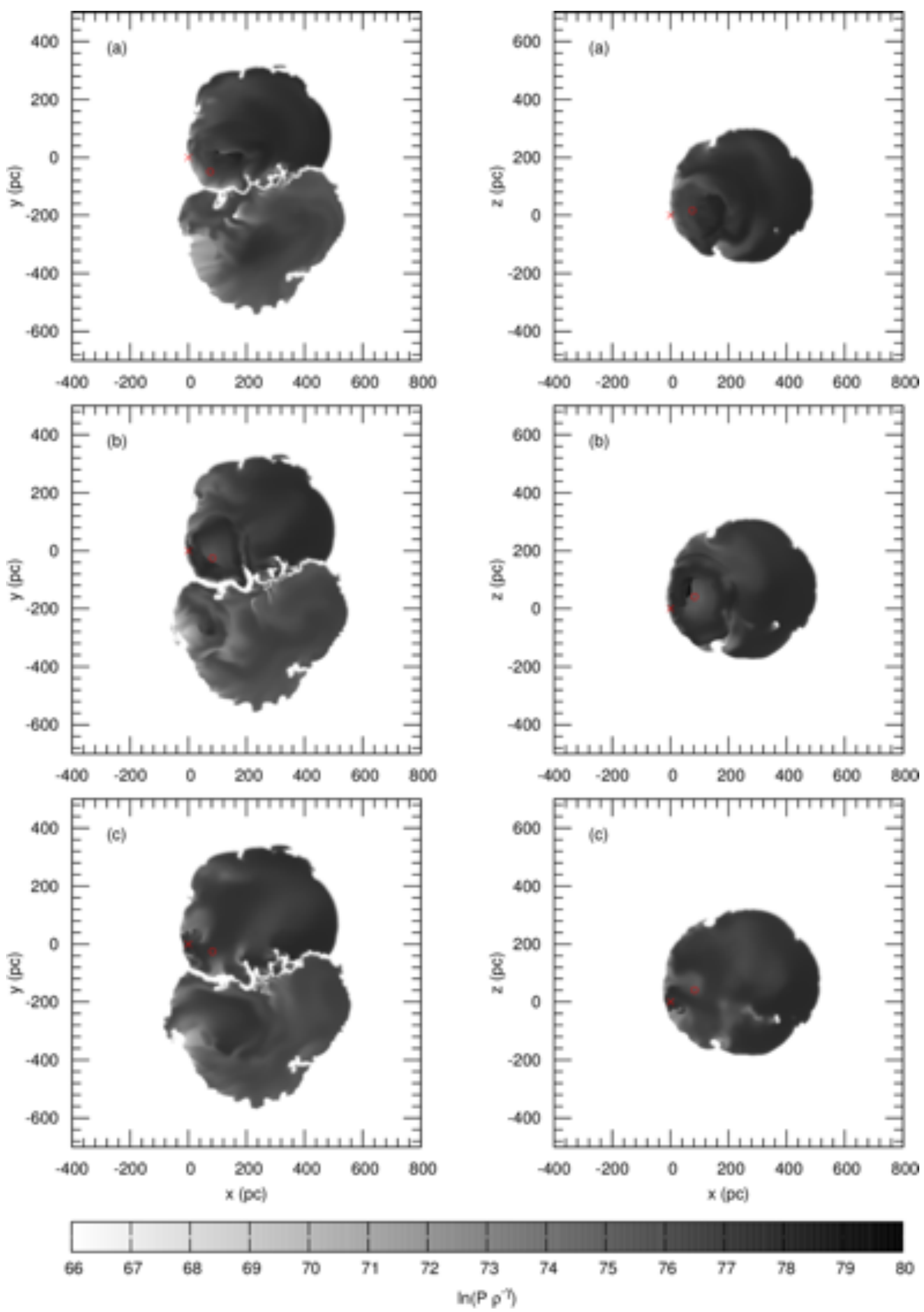

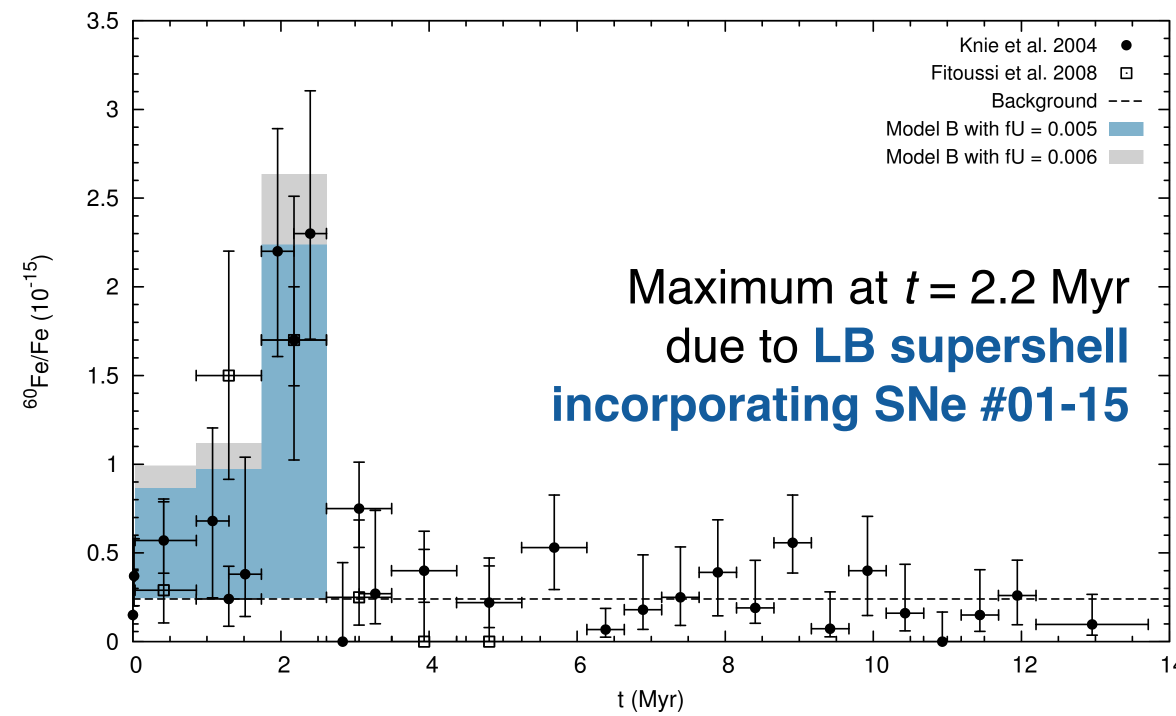

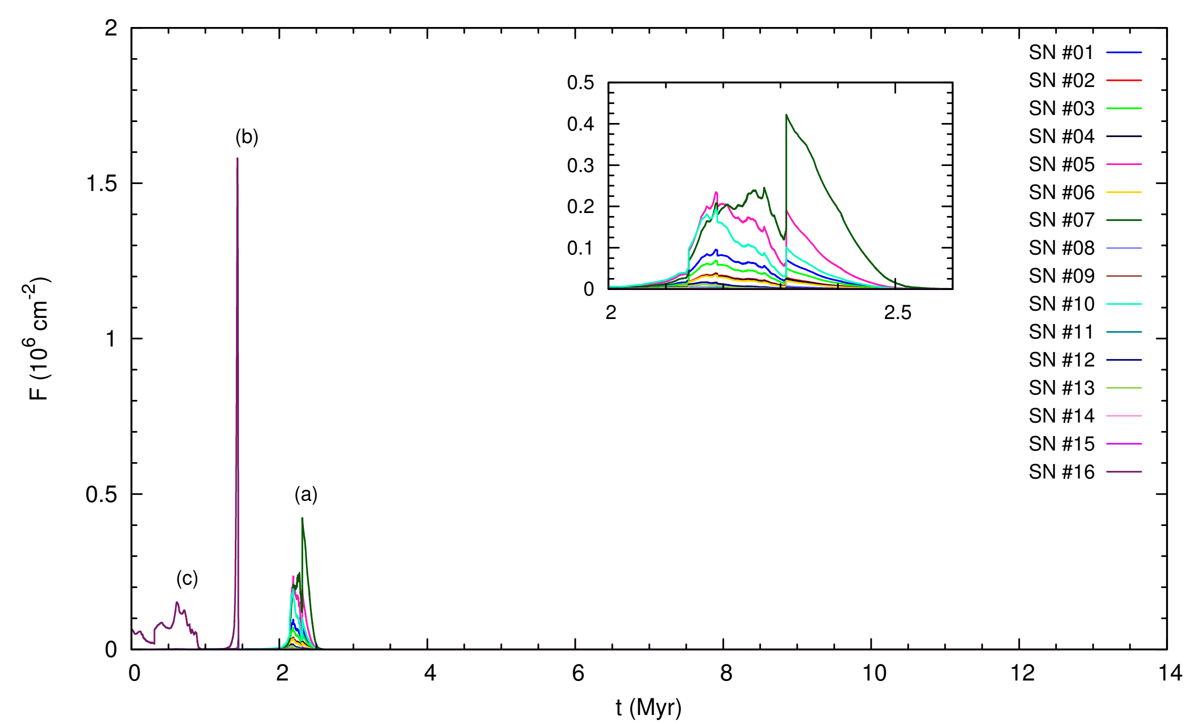

Results — Evolution of the Local Interstellar Medium

Atomic hydrogen number density and gas column density distribution (cuts through z = 0 and y = 0; 180 Myr evol. time)

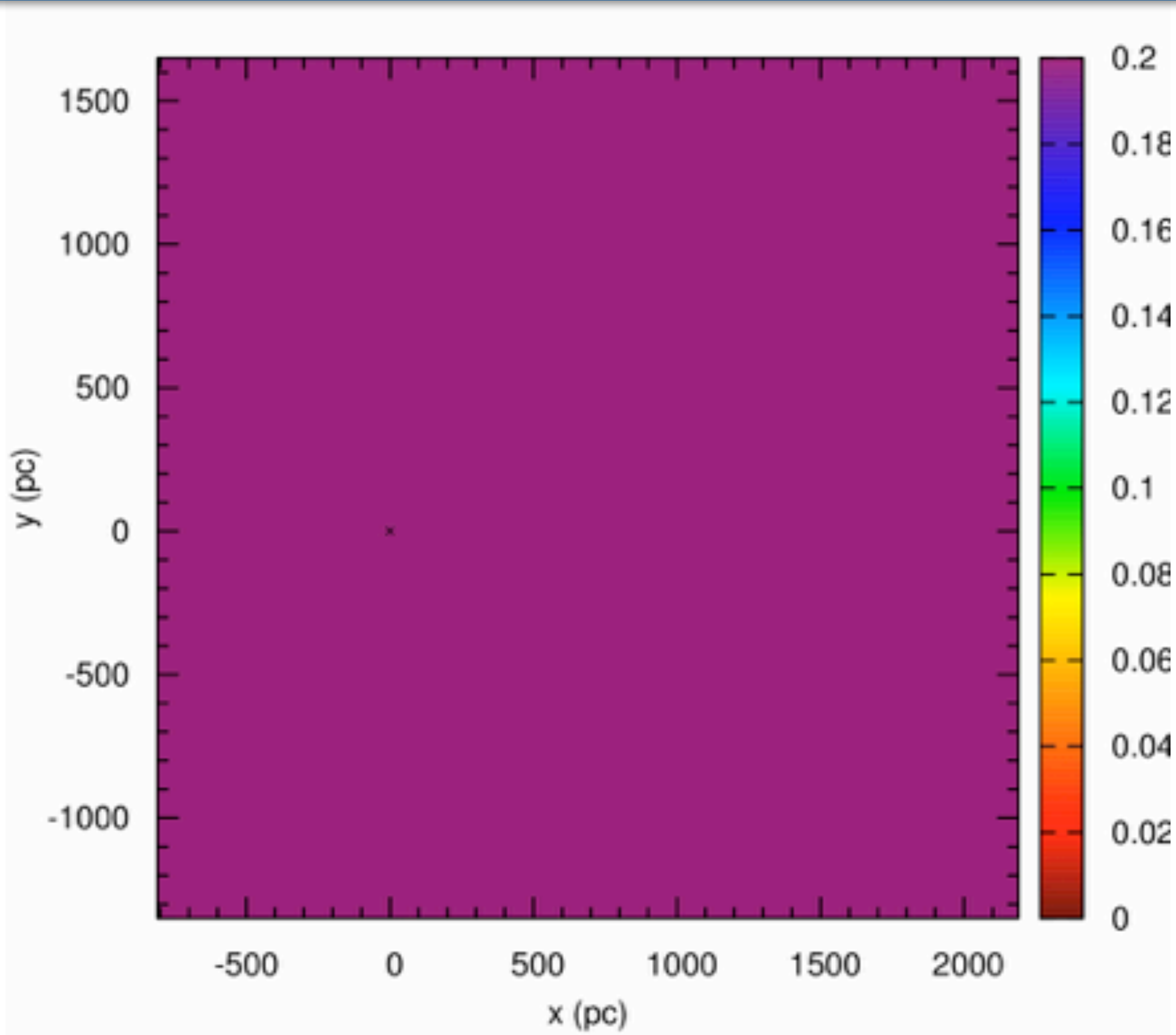

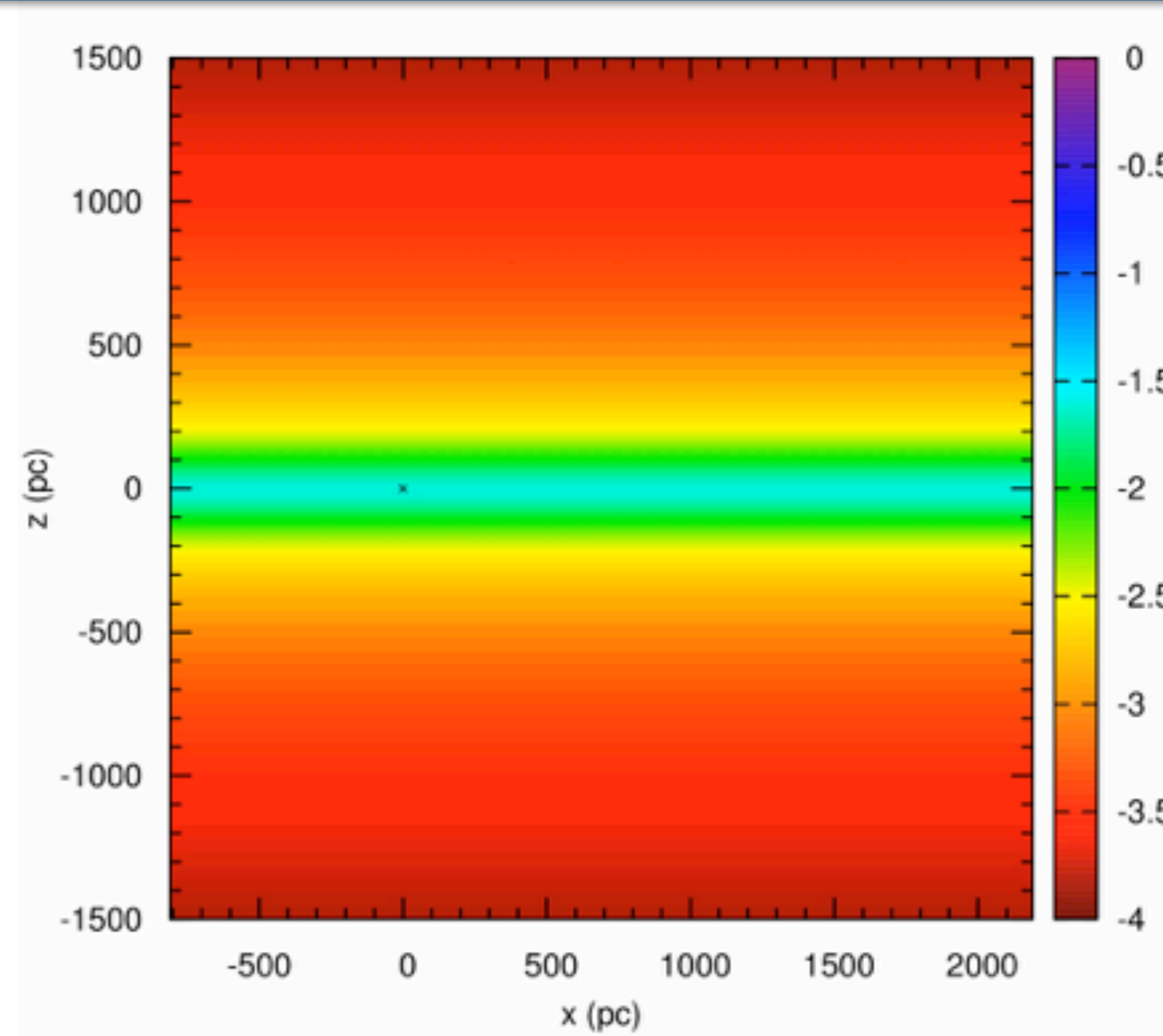

- **Initial distribution collapses** within first few Myr due to **imbalance between heating and cooling**
- Formation of **slab** with thickness 100-150 pc, comprising of major fraction of initial mass
- **Inhomogeneities** (enhanced by initially launched SNe) cool and compact further due to thermal instabilities -> **birth of first generation of massive stars**
- **Feedback processes** (winds, SNe, SBs) introduced by ongoing star formation provide pressure support needed by gas in slab to overcome gravitational pull and thus to **expand upwards**

- **After 180 Myr** (~ flow time ~ radiative cooling time; de Avillez & Breitschwerdt 2004): **quite extended clumpy disk of transient cold dense clouds (shock compressed layers) flanked by fountain flow in both hemispheres**
- Model does not reach dynamically steady state (volume filling factors of the disk |z| ≤ 250 pc do not converge; best fit with simulation of de Avillez & Breitschwerdt (2004) for t = 193 Myr; cold: 26%; cool: 42%; warm: 28%; hot: 4%)
  - **Reason:** Limited vertical extent of comp. box favours SN-driven **gas loss through cap boundaries**

Results — Chemical mixing simulations with inhomogeneous background medium

Model C: Evolution of the atomic hydrogen number density distribution (cuts through $z = 0$ and $y = 0$)

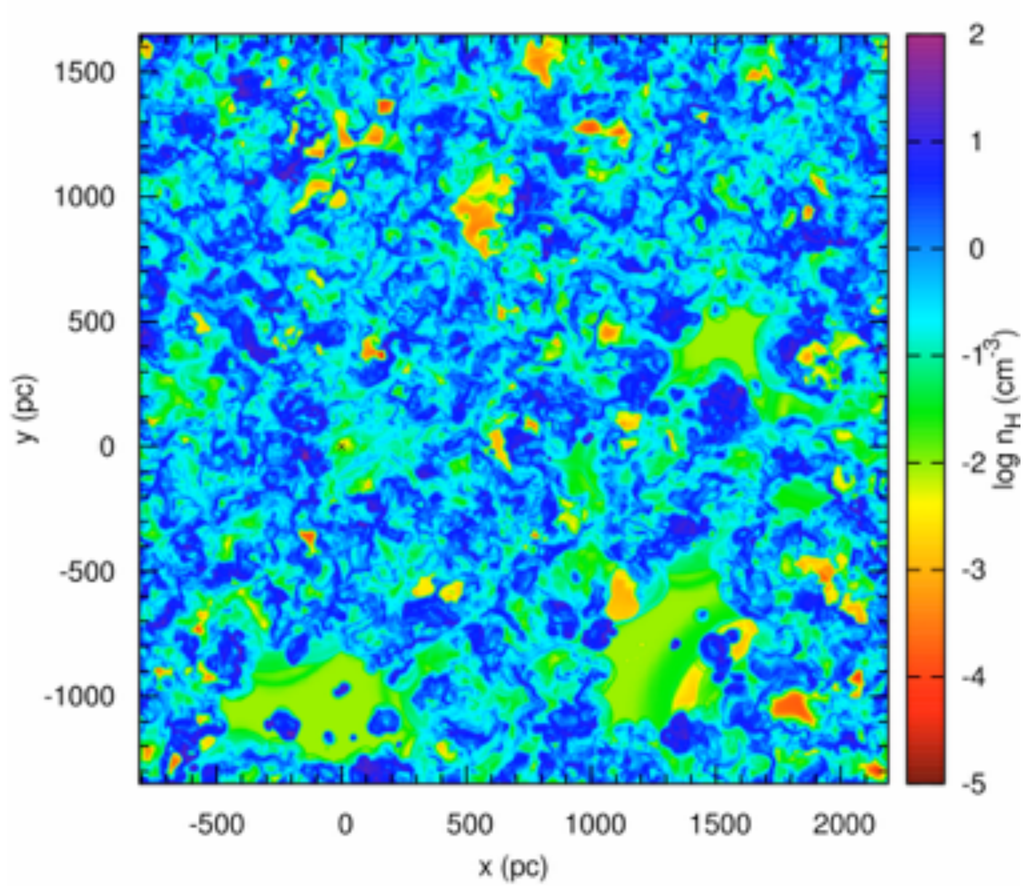

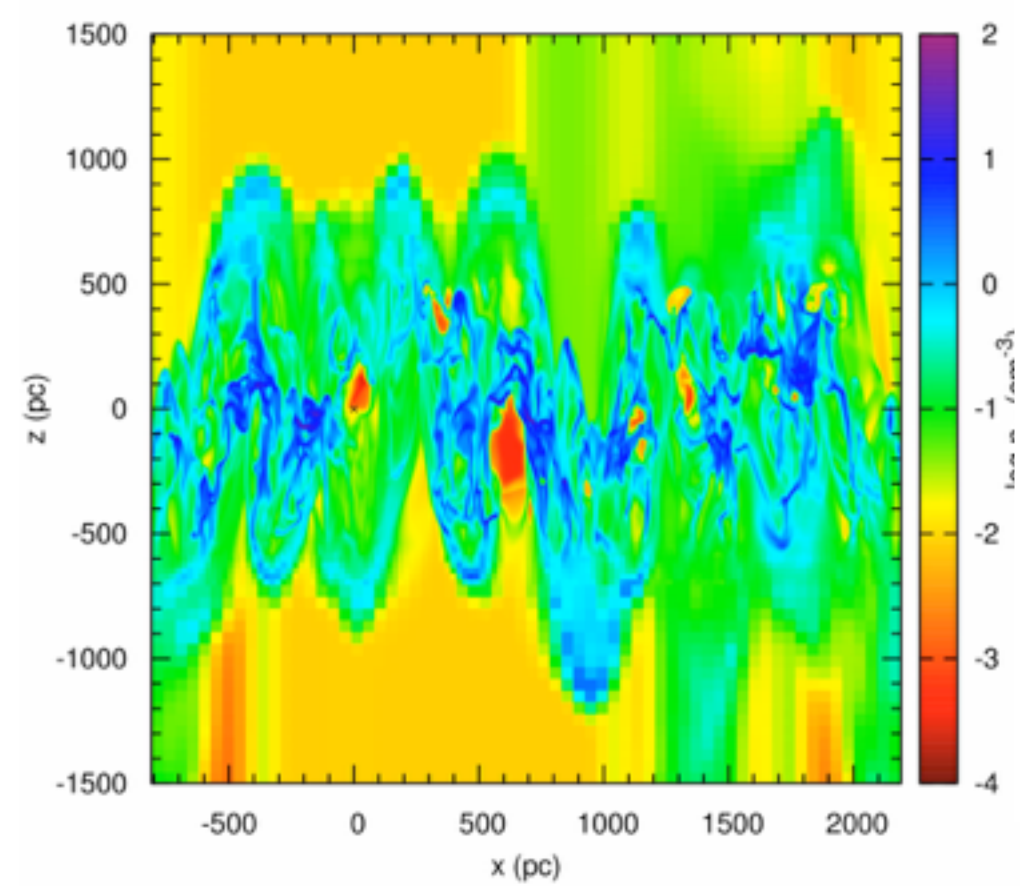

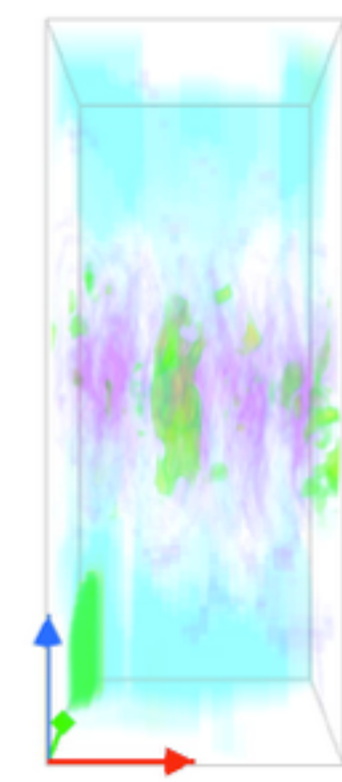

- Launch LB SNe in **suitable** environment
- search for extended region that remains sufficiently thin ($n \gtrsim 0.3\ \mathrm{cm}^{-3}$) at least for a few Myr
- no too strong vertical gas flows
- enough cold gas available for giving star cluster a plausible origin
- LB develops internal structures after ~8 Myr due to increasing influence of density/pressure gradients in the ambient medium

- 'Present' LB extension: $(x,y) = (280,260)$ pc, $|z| \gtrsim 500$ pc (northern half resembles chimney)
- Hydrogen density and temperature in 'present' LB cavity: $10^{-4.1}$-$10^{-2.2}$ cm^{-3}, $10^{4.5}$-$10^{6.5}$ K
- Loop I remains underdeveloped due to transient dense interstellar clouds in its domain ➔ no interaction shell

Results — Chemical mixing simulations with inhomogeneous background medium

Model C: Evolution of the ^{60}Fe mass density distribution (cuts through $z = 0$ and $y = 0$)

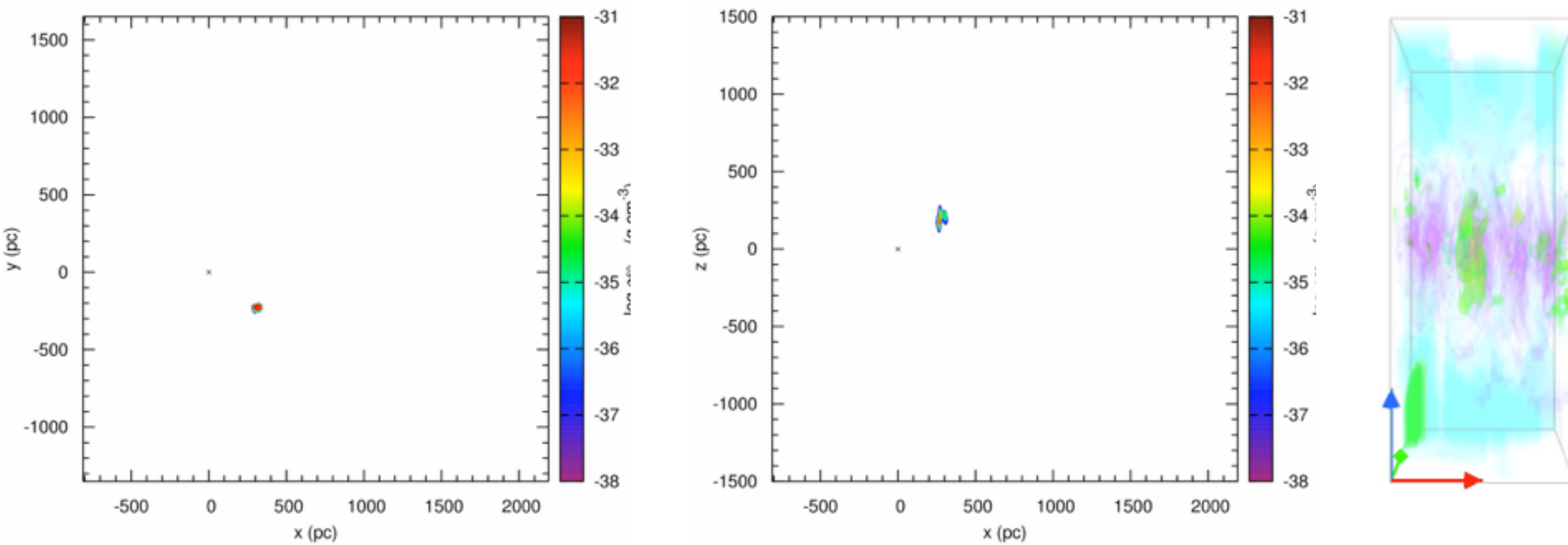

Only LB and Loop I are allowed to contribute to passive scalar field ➔ model gives lower limit of ^{60}Fe content of the local ISM.

Model C: Temporal variation of the local interstellar fluence of ^{60}Fe atoms and modeled $^{60}Fe/Fe$ content in the FeMn crust

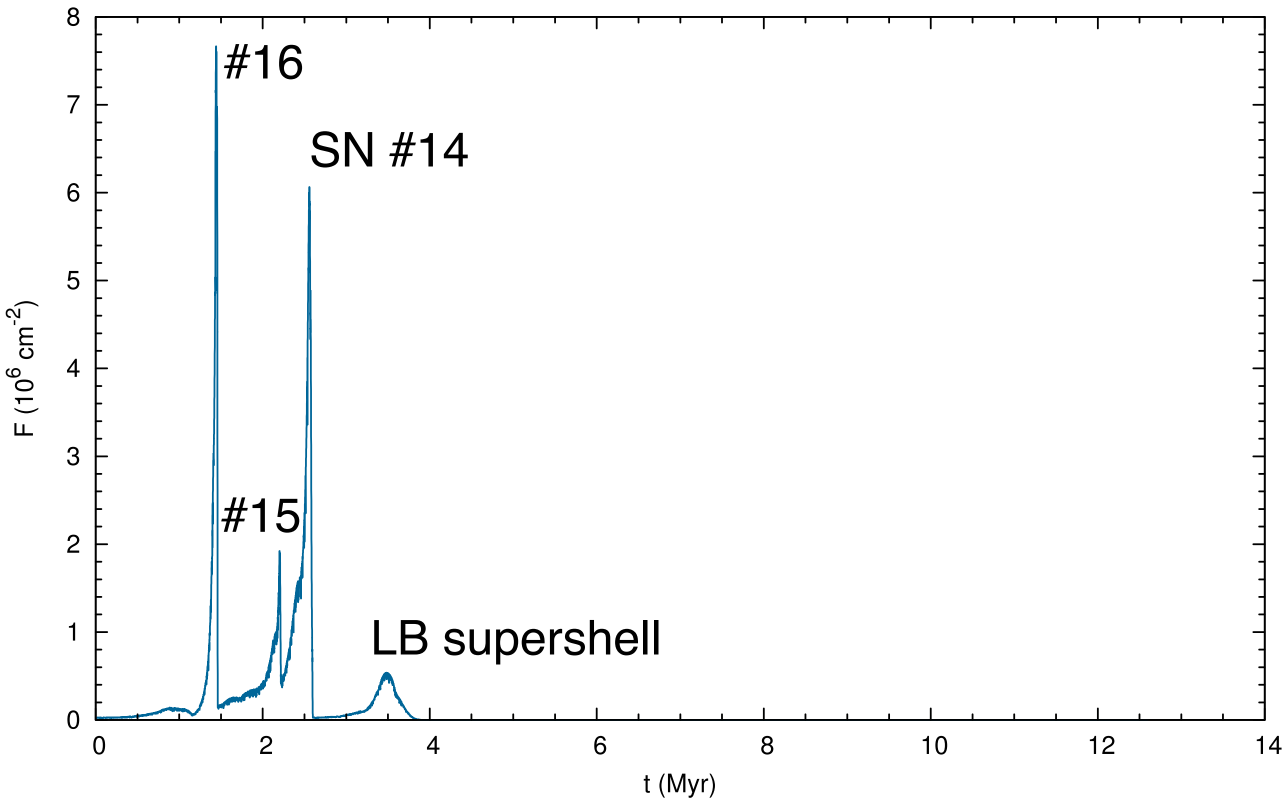

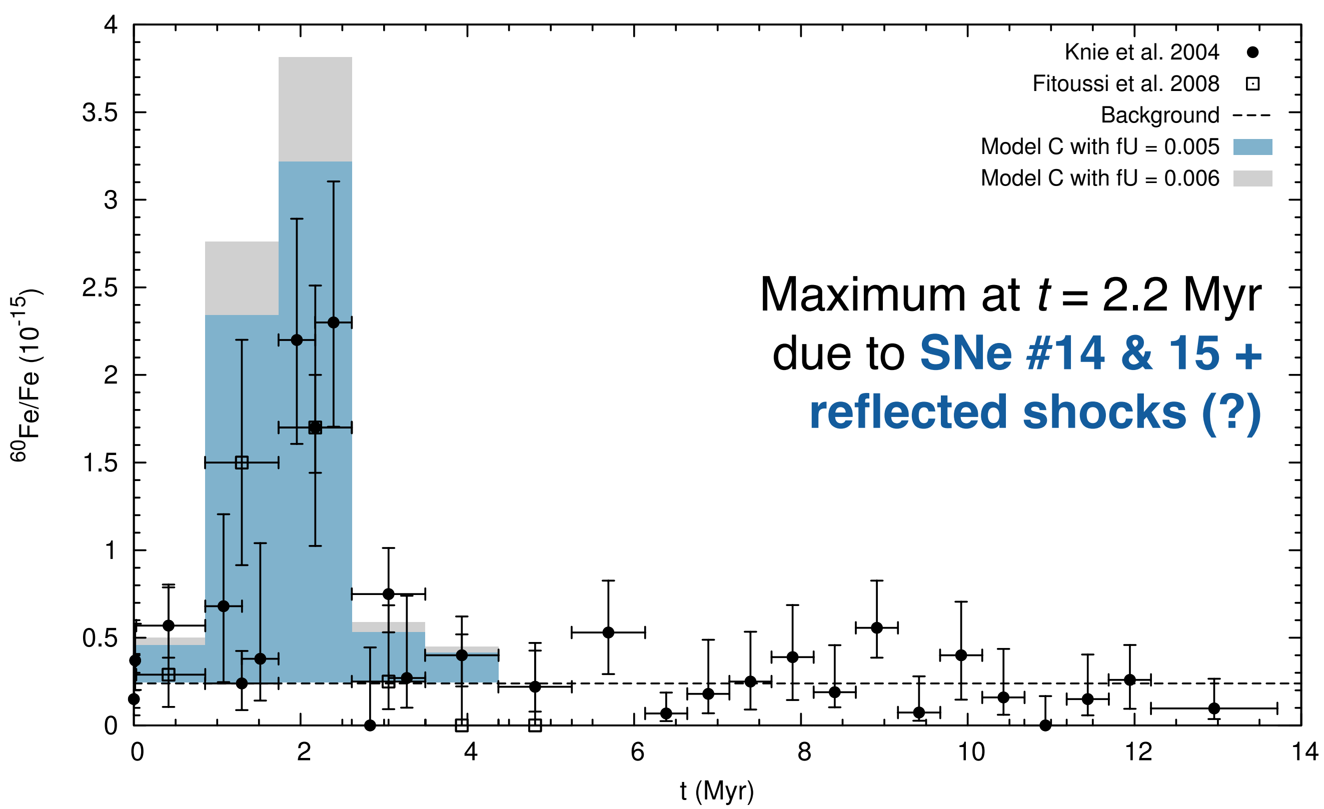

- Signal broadening due to four times lower numerical resolution
- Model C turns out to be a hybrid of model A and B:
  - Less signals due to individual SNe than in model A, but more than in model B
  - Mean density of the region where the LB evolves lies almost exactly in between model A and B [i.e., $(n)_{VA} \simeq 0.2$ cm^{-3}]
  - Supershell arrives later than in model A, but earlier than in model B ➔ self-gravity seem to play a rather subordinate role in LB evolution

Summary

- Our high-resolution hydrodynamical simulations show that the ^{60}Fe excess observed in a deep-sea FeMn crust can be attributed to nearby SNe that participated in the formation of the LB.
- SN parameters based on IMF are normalized to still existing low-mass stars of the stellar moving group, identified by Fuchs et al. (2006). Ejected masses, life/explosion times are derived from initial masses of the progenitor stars, explosion sites from calculations of the most probable paths of the perished moving group members. Recent stellar evolution models provide the particular ^{60}Fe mass ejecta, whose mixing is followed via passive scalars.
- The joint evolution of the Local and Loop I SB is studied in two homogeneous self-gravitating background media, similar to the classical WIM and WNM, as well as a medium designed to mimic more realistic conditions of the local Galaxy (i.e., SN-driven supersonic turbulence).
- Our model **reproduces both the timing and the intensity of the ^{60}Fe excess observed** with rather high precision. We identified **two alternative deposition agents**:
  - individual fast-paced SNRs, whose blast waves can get reflected from the LB's outer shell,
  - the LB shell itself that injects the isotopic content of all previous SNe at once, but over a longer time range.
- The LB properties observed are best matched by the model with inhomogeneous background medium.

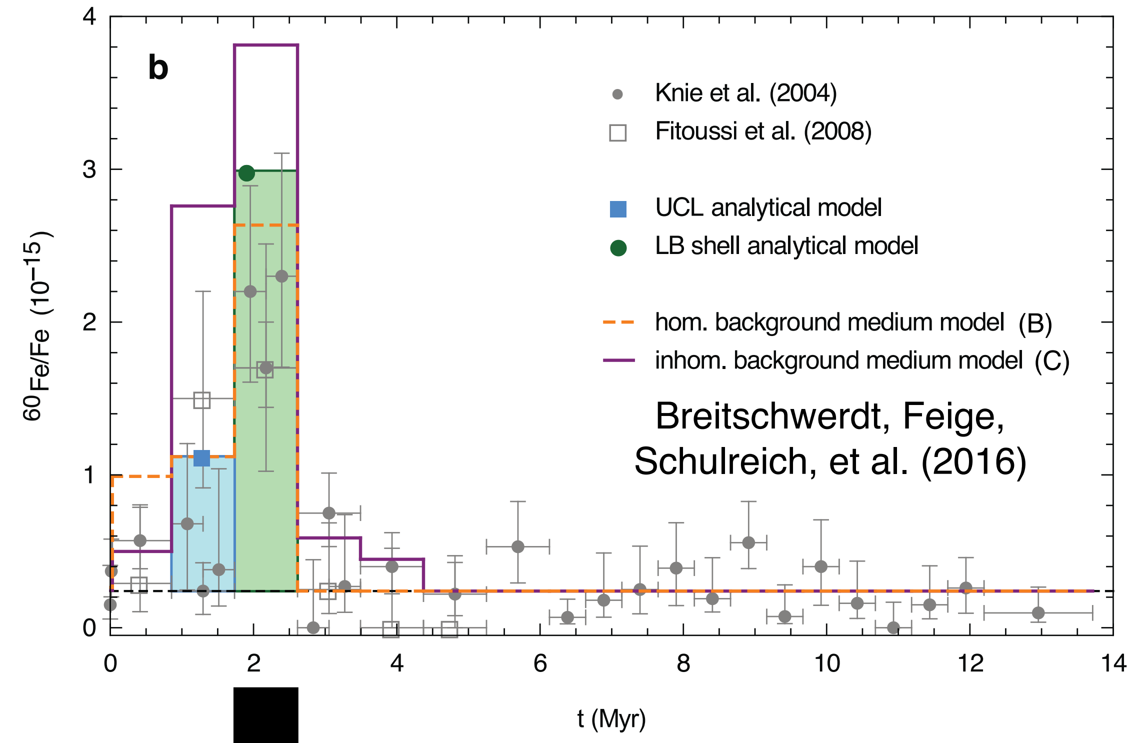

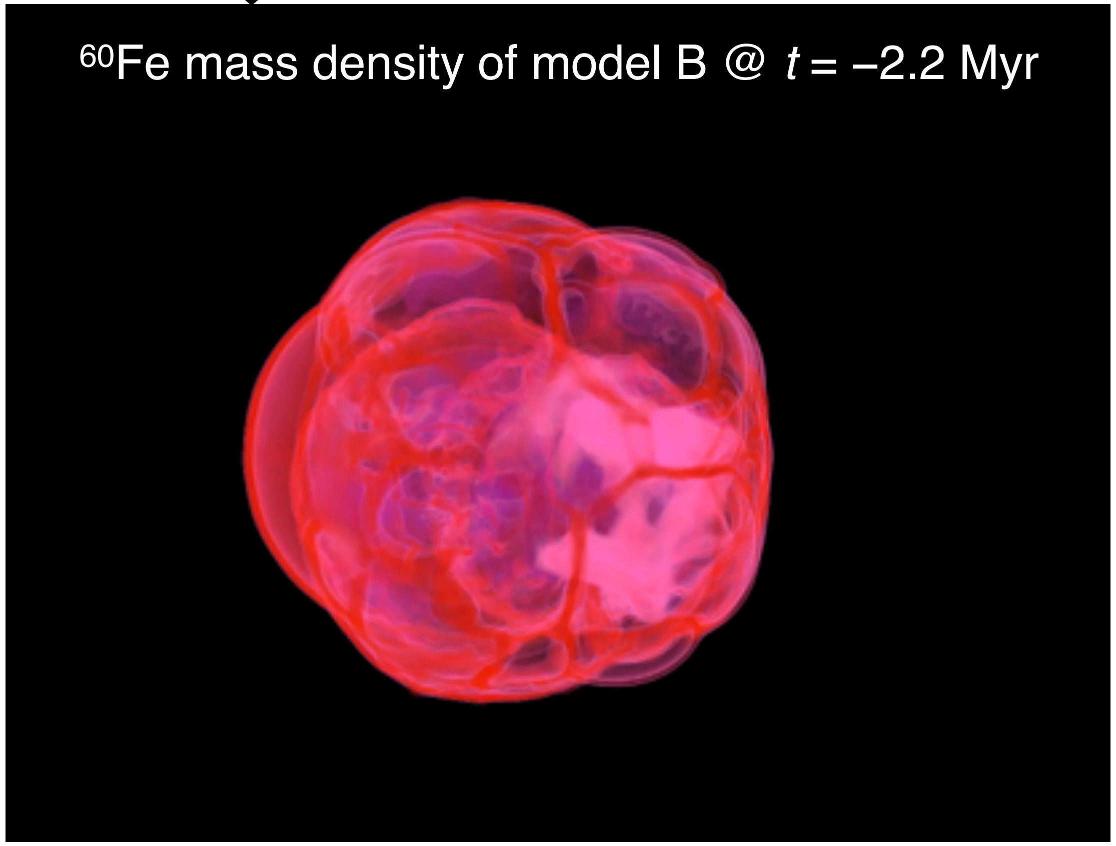

Outlook

Other terrestrial and extraterrestrial ^{60}Fe archives

1. Marine sediments

- Grow about thousand times faster than FeMn crusts ➔ better time resolution
- Formation process well understood ➔ uptake factor easily derivable (U ~ 1)
- Feige et al. (2012, 2014) & Wallner et al. (2016): sediment cores from South Australian Basin show signal consistent with expected time from FeMn crust study (^{60}Fe/Fe ~ 2 × 10^{-15}, on average); signal is broader (> 1.4 Myr) ➔ input of more than one SN

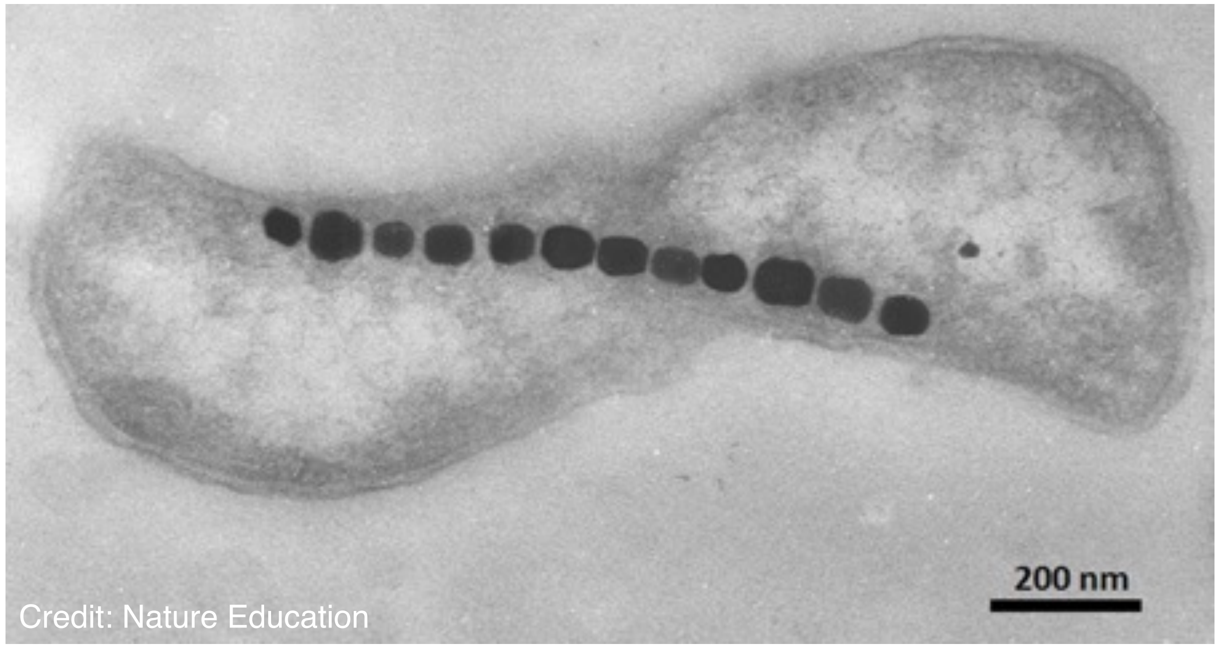

Credit: Nature Education

2. Magnetotactic bacteria

- Live in marine sediments
- Turn gathered iron into tiny crystals of magnetite
- Imprint of nearby SN event on fossilized remains of those bacteria?
- Bishop et al. (2013) indeed found minuscule levels of ^{60}Fe in microfossils from eastern equatorial Pacific Ocean, dating back to ~2.2 Myr ago


Credit: iStockphoto.com/narvikk

3. Lunar rocks

- Time-resolved measurements impossible due to 'gardening' and absence of sedimentation
- Cook et al. (2009) and Fimiani et al. (2012, 2014, 2016) found weak ^{60}Fe signal in Apollo samples ($F \sim 10^7$–6×10^7 cm^{-2}) ➔ **compatible with integrated fluence of our simulations** if, e.g., $U = 1$, $f = 0.016$

Neutron stars produced during LB formation process

Until now, no neutron star could be linked to ^{60}Fe anomaly (Tetzlaff et al. 2010, 2011); search goes on!

Further reading

- Breitschwerdt, D., Feige, J., Schulreich, M. M., de Avillez, M. A., Dettbarn, Ch. 2016, Nature, 532, 73
- Schulreich, M. M. et al. 2016a, A&A, in prep.
- Schulreich, M. M. et al. 2016b, A&A, in prep.

How Our Oceans Helped Reveal The Closest And Most Recent Exploding Stars To Earth
Buzzfeed

Attack of the stars: Radioactive debris from ancient supernova battered Earth millions of years ago
International Business Times (UK)

Finding the Earth-bound evidence for supernovae in the galactic neighbourhood
physicsworld.com

Proof that ancient supernovae zapped Earth sparks hunt for after effects
phys.org

Exploding Stars Spat Radioactive Debris All Over Earth
National Geographic

Supernova Fallout Hit Earth When Human Ancestors Were Alive
Air & Space

Exploding stars left recent, radioactive mark on Earth
BBC News

Radioactive material in ocean crusts likely came from nearby star explosions
The Verge

Ancient exploding stars hurled radioactive debris at Earth — and it's still here
Washington Post

Future work

Wallner et al. 2016, Nature, 532, 69:

- Analyzed deep-sea archives from all major oceans
- Found that ^{60}Fe signal is global **and extended in time** (1.5–3.2 Myr ago) ➔ **multiple-SN origin**, as suggested by our models
- Detected **additional '^{60}Fe bump'** at 6.5–8.7 Myr ago
- Further constraint for our LB formation scenario ➔ earlier arrival of LB supershell?

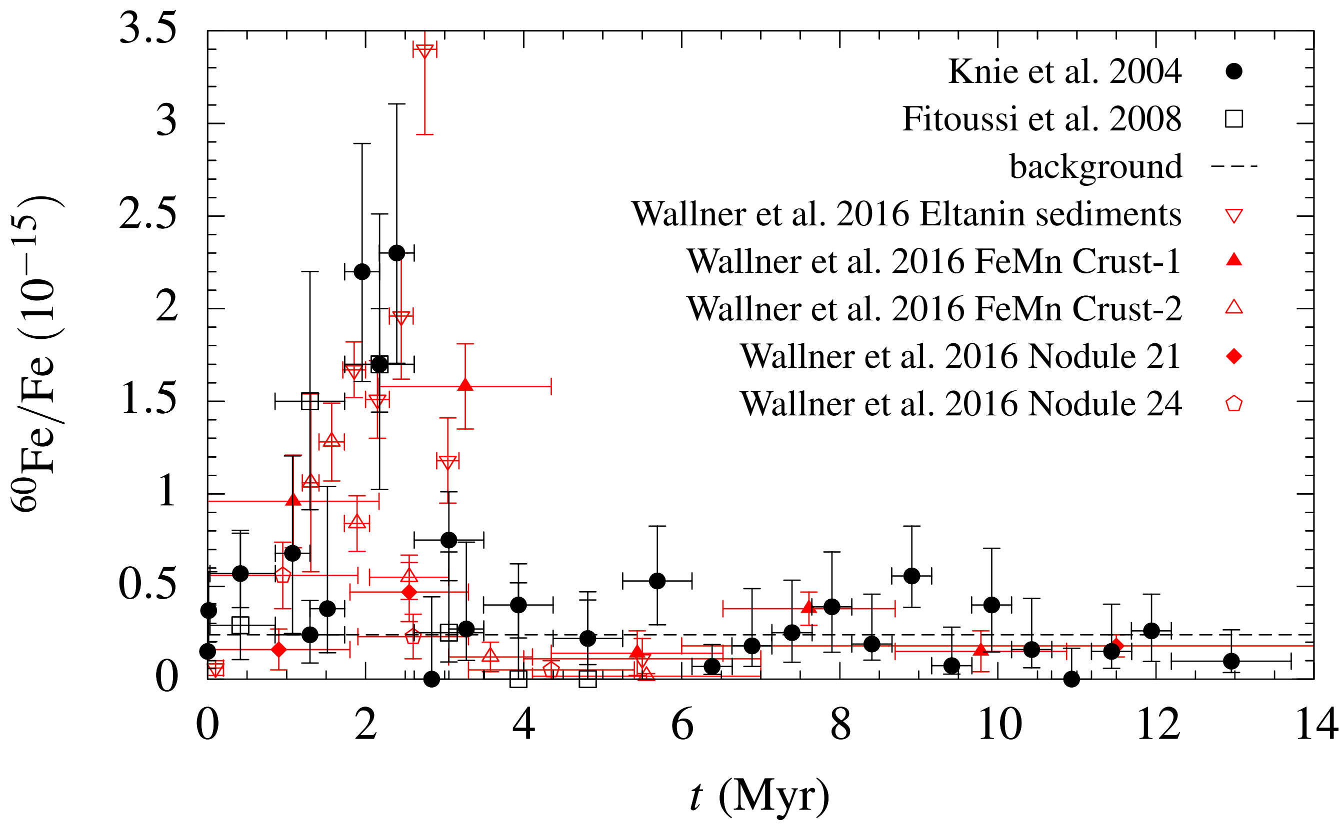

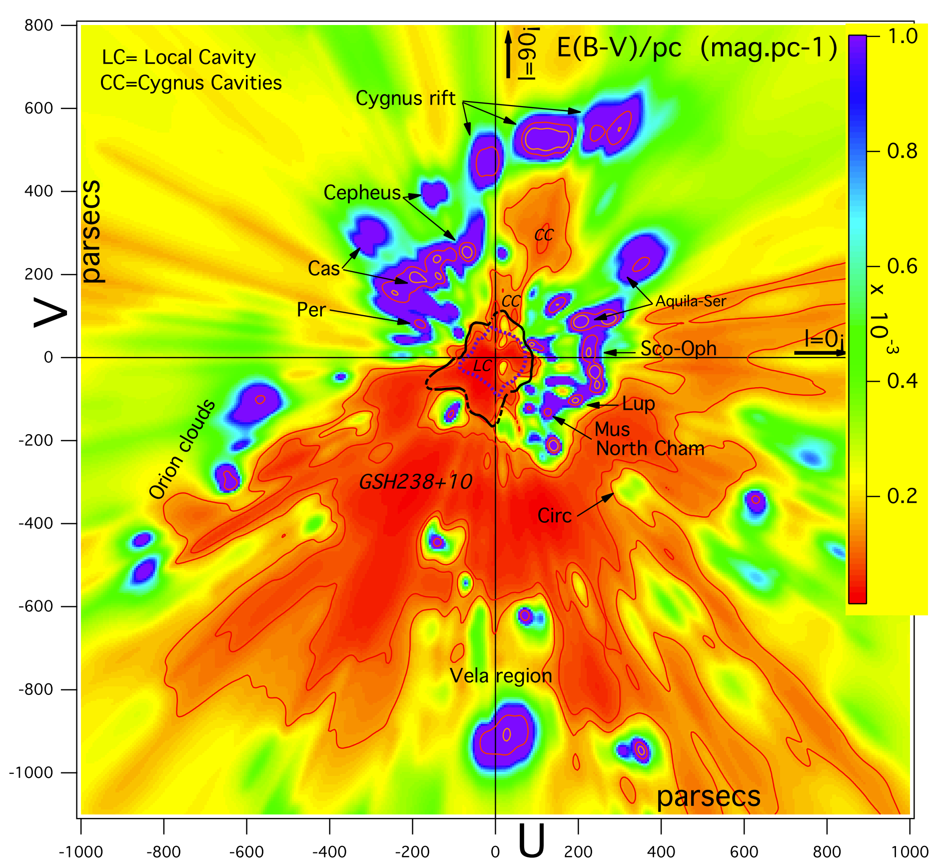

Use actually observed background medium: Extended and highly resolved maps of the local ISM from Lallement et al. 2014

- Created from inverting ~23,000 redding measurements toward nearby stars
- Limited number of target stars ➔ smoothing length (structures smaller than 15 pc are not mapped at their actual sizes)
- Black contour line: ROSAT unabsorbed 0.25 keV surface brightness (Snowden et al. 1998)
- Blue contour line: averaged estimated heliospheric contribution to the signal (Puspitarini et al. 2014)

Parameters for Local Bubble supernovae

t_{SN}	m ($M_\odot$)	M_{ej} (10^{-5} $M_\odot$)	x (pc)	y (pc)	z (pc)	D (pc)	l (°)	b (°)	α	δ	sc
-12.6[2]	19.86	6.3	277	75	89	300	15.15	17.23	17^h17^m	$-7°09^m$	Oph
-12.0[3]	18.61	5.5	223	99	71	254	23.94	16.22	17^h37^m	$-0°21^m$	Oph
-11.3[2]	17.34	5.0	251	67	87	274	14.95	18.52	17^h12^m	$-6°39^m$	Oph
-10.0[2]	15.41	4.2	227	57	83	248	14.10	19.53	17^h07^m	$-6°48^m$	Oph
-10.0[3]	15.36	4.1	185	77	67	211	22.60	18.49	17^h27^m	$-0°23^m$	Oph
-8.7[2]	13.89	3.6	203	45	79	222	12.50	20.80	17^h00^m	$-7°23^m$	Oph
-8.0[3]	13.12	3.4	151	49	57	169	17.98	19.75	17^h14^m	$-3°34^m$	Oph
-7.5[2]	12.65	3.3	181	31	75	198	9.72	22.22	16^h49^m	$-8°46^m$	Oph
-6.3[2]	11.62	3.0	163	11	73	179	3.86	24.10	16^h30^m	$-12°03^m$	Oph
-6.1[3]	11.48	2.9	121	19	47	131	8.92	20.99	16^h52^m	$-10°04^m$	Oph
-5.0[2]	10.76	2.7	145	-5	69	161	-1.97	25.43	16^h12^m	$-15°19^m$	Sco
-4.2[3]	10.21	2.6	97	-15	33	104	-8.79	18.58	16^h16^m	$-24°35^m$	Sco
-3.8[2]	10.02	2.6	125	1	51	135	0.46	22.19	16^h28^m	$-15°40^m$	Oph
-2.6[2]	9.37	2.4	95	-9	47	106	-5.41	26.22	16^h01^m	$-17°05^m$	Lib
-2.3[3]	9.21	2.4	75	-49	17	91	-33.16	10.74	15^h10^m	$-45°35^m$	Lup
-1.5[2]	8.81	2.3	83	-25	41	96	-16.76	25.31	15^h32^m	$-24°44^m$	Lib